

Visual Field Maps in Human Cortex

Brian A. Wandell,^{1,*} Serge O. Dumoulin,¹ and Alyssa A. Brewer²

¹Psychology Department, Stanford University, Stanford, CA 94305-2130, USA

²Department of Cognitive Sciences, University of California, Irvine, Irvine, CA 92697, USA

*Correspondence: wandell@stanford.edu

DOI 10.1016/j.neuron.2007.10.012

Much of the visual cortex is organized into visual field maps: nearby neurons have receptive fields at nearby locations in the image. Mammalian species generally have multiple visual field maps with each species having similar, but not identical, maps. The introduction of functional magnetic resonance imaging made it possible to identify visual field maps in human cortex, including several near (1) medial occipital (V1,V2,V3), (2) lateral occipital (LO-1,LO-2, hMT+), (3) ventral occipital (hV4, VO-1, VO-2), (4) dorsal occipital (V3A, V3B), and (5) posterior parietal cortex (IPS-0 to IPS-4). Evidence is accumulating for additional maps, including some in the frontal lobe. Cortical maps are arranged into clusters in which several maps have parallel eccentricity representations, while the angular representations within a cluster alternate in visual field sign. Visual field maps have been linked to functional and perceptual properties of the visual system at various spatial scales, ranging from the level of individual maps to map clusters to dorsal-ventral streams. We survey recent measurements of human visual field maps, describe hypotheses about the function and relationships between maps, and consider methods to improve map measurements and characterize the response properties of neurons comprising these maps.

Introduction

Modern neuroscience emphasizes the principle that human perception is determined by the properties of brain circuitry. It is equally important to recognize that these brain circuits evolved to interpret the properties of the physical environment (Shepard, 1981, 2001). This relationship between the physical environment and brain circuitry has been recognized by many important investigators. Newton discussed the separation of the physical stimulus and psychological interpretation: “The rays, to speak properly, are not colored. In them there is nothing else than a certain power... to stir up a sensation of this or that color.” (Newton, 1704). Helmholtz wrote that neural circuitry and perceptual experience are organized to estimate the physical signal: “*such objects are always imagined as being present... as would have to be there in order to produce the same impression on the nervous mechanism*” (Helmholtz, 1896, italics in original).

The most important physical property of the visual image is its spatial arrangement. One can alter the image contrast, change colors, tilt the image, or randomly remove small regions (pixels) and still recover a great deal of essential information about the image. But if one scrambles the spatial arrangement of the image at a fine scale any realistic chance of reconstructing the original is lost. Hence, we should not be surprised to find that the spatial representation of the image features is preserved and repeated multiple times within cortex. The multiplicity of visual field representations in cortex appears to reflect an accommodation between this quintessential image property and the neural circuitry's structure. As cortex interprets different aspects of the visual image—such as its

spectral composition, motion, and orientation—the cortical circuitry is organized using receptive fields that preserve the most critical image information, its spatial organization. Hence, regions of visual cortex with a variety of visual functions still preserve the visual field map.

The Size and Location of Human Visual Cortex

Each hemisphere of human cortex spans a surface area on the order of 1000 cm² (Van Essen, 2007) and ranges between 2–4 mm in thickness (Blinkov and Glezer, 1968; Braitenberg and Schüz, 1998; Fischl and Dale, 2000). Each cubic millimeter of cortex contains roughly 50 thousand neurons (Braitenberg and Schüz, 1998), so assuming an average thickness of 2.5 mm, the two cortical hemispheres contain on the order of 25 billion neurons (Pakkenberg and Gundersen, 1997).

Modern neuroimaging experiments demonstrate that much of the posterior human brain responds to visual stimulation. Human visual cortex includes the entire occipital lobe and extends significantly into the temporal and parietal lobes (Figure 1A), spanning about 20% of cortex. Hence, human visual cortex contains on the order of 5 billion neurons. Assigning sensory and motor functions to distinct cortical regions was a contentious scientific debate (Phillips et al., 1984). Munk was the first to reach the conclusion that “The visual center of the monkey is the cortex of his occipital lobe [...]. Only injuries of this cortex lead to disturbances of the visual sense and only such disturbances follow lesions of this cortex.” (Munk, 1881). By performing localized lesion experiments in mammalian cortex, he further showed the presence of a visual field map (Russell, 2001). Henschen (1893) subsequently reviewed cases of visual loss in human and identified the

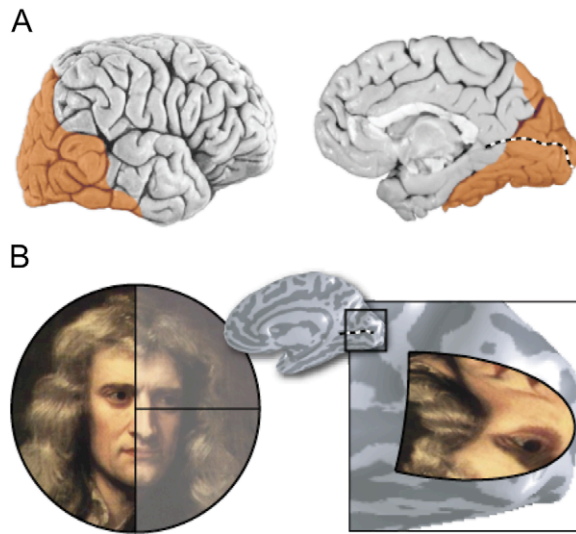


Figure 1. Human Visual Cortex and V1 Visual Field Map

(A) Human visual cortex (orange overlay) occupies approximately 20% of the cerebral cortex and is located in the occipital lobe and posterior parts of the parietal and temporal lobes. Primary visual cortex (V1) is located in and around the calcarine sulcus (dotted line) and contains a map of the visual field.

(B) We illustrate the visual field map in V1. The image is a section of Godfrey Kneller's 1689 portrait of Sir Isaac Newton. The figure illustrates how the visual field (left) is transformed and represented on the V1 cortical surface (right) using a mathematical description proposed by Schwartz (1977). The left visual field stimulates V1 in the right hemisphere; the image representation is inverted, and the center of the visual field, near the eye, is greatly expanded (cortical magnification).

calcarine sulcus, located on the medial aspect of the occipital lobe, as essential for vision.

The Discovery of Visual Field Maps

More than a century ago Inouye, an ophthalmologist, and then Holmes, a neurologist, observed strong correlations between visual field deficits and the location of lesions within human visual cortex (V1) (Fishman, 1997; Holmes, 1918; Inouye, 1909; Teuber et al., 1960). Their analyses of these correlations defined the visual field map in human primary visual cortex, V1, and established several important principles. They showed that V1 in each hemisphere encodes a hemifield (i.e., one half of visual space) and that the central fovea is represented over a larger fraction of cortical surface than a comparable extent of the peripheral visual field (cortical magnification, Figure 1B). These neurological maps were useful guides for many generations of clinicians and have only recently been revised (Horton and Hoyt, 1991).

Importantly, subsequent animal experiments uncovered multiple maps. In the 1940s electrophysiological measurements revealed a second map (V2) adjacent and surrounding V1 in rabbit and cat (Talbot and Marshall, 1941; Talbot, 1940, 1942; Thompson et al., 1950; Tusa et al., 1978) and then later in squirrel monkey (Cowey, 1964). A third map (V3) adjacent and surrounding V2 was then described in cat (Hubel and Wiesel, 1965). In the 1970s, investigators

described additional visual field maps in monkey, including one (V4) adjacent to V1/2/3 and another located at some distance from this first posterior group (MT/V5) in owl monkey (Allman and Kaas, 1971). Zeki described a framework for the concentric organization of these maps in macaque (Gattass et al., 2005; Zeki, 1969, 1971, 1976). During the 50 years from 1940 to 1990, the number of reported visual field maps grew enormously, and investigators began to hypothesize about the organization among the maps themselves (Felleman and Van Essen, 1991; Goodale and Milner, 1992; Milner and Goodale, 2006; Ungerleider and Mishkin, 1982; Van Essen and Maunsell, 1983).

The organization and perceptual significance of the human V1 map were confirmed by experiments showing that local electrical stimulation in the V1 map gives rise to a sensation of light (phosphene) at the corresponding visual field location (Brindley and Lewin, 1968). The V1 map was measured in the living human brain using positron emission tomography (PET) (Fox et al., 1987). But it was only in the early 1990s with the introduction of fMRI (Ogawa and Lee, 1990; Ogawa et al., 1990, 1992) and novel data-analysis methods (Engel et al., 1994) that investigators could measure efficiently multiple visual field maps in the intact human visual cortex (DeYoe et al., 1996; Engel et al., 1997; Sereno et al., 1995). Subsequent advances in magnetic resonance instruments, experimental methods, and data analysis algorithms produced a significant amount of new data about the organization of human visual field maps (Figure 2). The main purpose of this review is to summarize the recent visual field map measurements in human cortex.

The Motivation for Measuring Human Visual Field Maps

fMRI measurements of human visual field maps are being actively explored because of the strong interest in the human brain and the likelihood of clinical applications. Differences between primate species (Rosa and Tweedale, 2005) and differences between human and nonhuman primates (Brewer et al., 2002; Tootell et al., 1997; Van Essen, 2003) make the direct measurements of human cortex essential.

The delineation of human visual field maps serves multiple goals. First, visual neuroscience theory postulates that cortical regions are specialized for specific perceptual functions. This general principle is supported by neurological cases showing that localized damage can lead to very specific visual deficits, such as achromatopsia, prosopagnosia, or akinetopsia (Zeki, 1993). The idea that specific visual field maps serve certain perceptual specializations is supported by both the observation that certain maps are comprised of a set of neurons with common stimulus selectivity and that stimulation of these neurons within a map specifically influences behavior. For example, stimulation of the direction-selective neurons in area MT specifically influences behavioral decisions about motion in specific directions and visual field positions (Salzman et al., 1990, 1992). The relationship between maps and perceptual function is neither direct nor unique: it is likely that

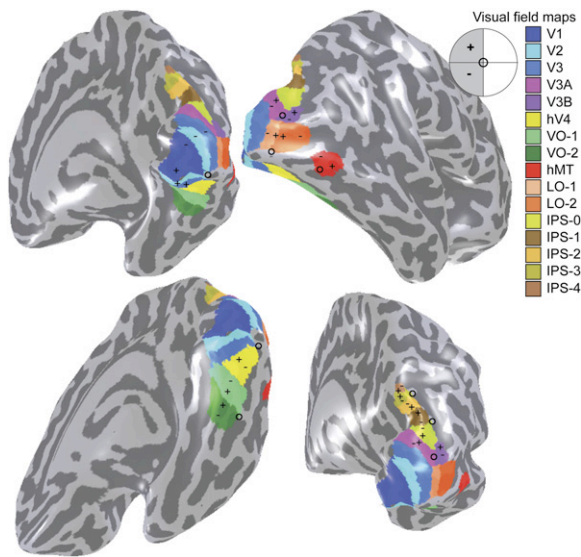


Figure 2. Visual Field Maps in Human Visual Cortex

The positions of sixteen maps are shown on an inflated rendering of the cortical surface of a right hemisphere. Although this organization is generally accepted, certain aspects are still debated. Most of the visual field maps are based on measurements of one subject (V1/2/3, hV4, VO-1/2, LO-1/2, IPS-0); others are added based on descriptions in the literature (IPS-1/2/3/4, hMT). Fovea and upper/lower visual fields are indicated by the “o”, “+”, and “-” symbols, respectively. The posterior visual maps in and around calcarine are labeled V for visual and a number, e.g., V1, V2, V3, V3A, following the naming of homologs in macaque monkey. To be conservative about potential homology between these maps and maps in nonhuman primates, we use a conservative labeling scheme. Maps in lateral occipital are numbered as LO-x, maps in ventral occipital are numbered as VO-x, and maps in the intraparietal sulcus are numbered IPS-x.

more than one map is essential for a particular visual function and that each individual map participates in multiple functions. Characterizing the responses within specific visual field maps is an essential task in understanding the cortical organization of visual functions.

Second, the visual field map provides useful information about the likely perceptual function of a specific cortical region. For example, field maps define the amount of cortical surface area allocated as a function of visual field eccentricity, a measure commonly called cortical magnification (Daniel and Whitteridge, 1961) (see Figure 1B). Some cortical visual field maps are principally devoted to processing foveal information, others less so (Dougherty et al., 2003; Ejima et al., 2003; Engel et al., 1997; Pitzalis et al., 2006; Sereno et al., 1995). Such differences in cortical magnification may correlate with differences in perceptual processing requirements (Malach et al., 2002).

Third, quantitative measurements of these maps can be used for detailed analyses of visual system pathologies (Barnes et al., 2001; Baseler et al., 1999, 2002; Morland et al., 2001; Sunness et al., 2004; Victor et al., 2000). Visual field map changes can be used to track cortical reorganization following retinal or cortical injury (plasticity). Further, if we are to identify cortical changes underlying visual dysfunction and perceptual deficits, we need to have

baseline measurements of features such as visual field map size and organization.

Fourth, quantitative measurements are a good basis for interspecies comparisons (Van Essen, 2002, 2003). There is a wealth of literature from primate measurements from which it is useful to draw information for human studies, but an understanding of the homology across the species is necessary. If we are to identify homologous regions securely, it is best to have quantitative measurements from both species. We discuss questions of homology in more detail in the section *Monkey and Human Visual Field Maps*.

Finally, visual field maps provide a useful way to compare or combine responses of individual observers or groups of observers. Without knowledge of the functional maps, functional responses can be compared only by identifying common anatomical landmarks. But the human brain's anatomical structure is highly varied, and methods for placing a brain within a stereotaxic coordinate system, such as Talairach (Talairach and Tournoux, 1988) or MNI space (Collins et al., 1994), rarely provide spatial certainty within half a centimeter (Di Russo et al., 2002; Iaria and Petrides, 2007; Thompson et al., 1996). Furthermore, alignment of gross anatomical features will not necessarily align cytoarchitectonic (Rademacher et al., 1993) or functional regions (Dumoulin et al., 2000). Identifying a region-of-interest (ROI) using a functional measurement, such as a map, provides much better support for the assumption that one is measuring comparable regions across individuals. There is an interesting debate about the value of ROI measurements and the optimal implementation of localizer scans (Friston et al., 2006; Saxe et al., 2006). This debate focuses on stimulus-specific ROIs defined by thresholding signal amplitudes elicited by viewing particular stimuli, such as fusiform face area (Kanwisher et al., 1997) and lateral occipital complex (Malach et al., 1995). However, unlike these stimulus-specific ROIs, the value of visual field maps for identifying common regions in different observers is acknowledged by both sides. Indeed, identification of visual field maps is a prerequisite for many neuroimaging studies of human visual cortex.

Measuring Visual Field Maps

Visual field maps are defined with respect to the fixation point. Stimuli to the right of fixation are in the right visual field, stimuli above fixation are in the upper field, and so forth. Because the visual field shifts with the eye position but is fixed with respect to the retina, visual field maps are also called *retinotopic maps*.

Traveling-Wave Method

Visual field maps measure the stimulus location that causes the largest response at each cortical position (Figure 3). Many laboratories use the traveling-wave method (also called phase-encoded retinotopic mapping) (Engel et al., 1994) with ring and wedge stimuli to measure visual field maps (DeYoe et al., 1996; Dumoulin et al., 2003; Engel et al., 1997; Sereno et al., 1995; Wandell et al., 2005; Warnings et al., 2002). In this method, a fixating observer

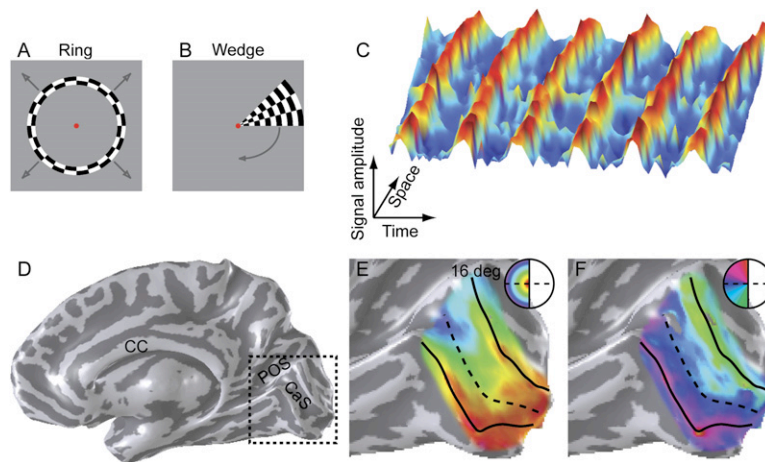


Figure 3. Traveling-Wave Method

Traveling-wave stimuli comprise a set of contrast patterns at different eccentricities or angles. We show an example of one stimulus frame from the expanding ring (A) and rotating wedge (B) stimulus sequence. The arrows indicate the direction in which the contrast pattern sections are moving in sequential stimulus frames, but the arrows are not present in the stimulus. These stimuli elicit a BOLD signal modulation on the order of 1%–3%. (C). This modulation is typically 15–20 standard deviations above the background noise. The time (phase) of the peak modulation varies smoothly across the cortical surface (space). Six stimulus repetitions are shown. In this case, space measures distance along the calcarine sulcus in the right hemisphere (indicated by the dashed lines in panels E and F). The time delay (phase) defines the most effective stimulus eccentricity (ring) and angle (wedge) in the stimulus sequence. The inflated cortical surface (D)

is labeled as follows: corpus callosum, CC; the parietal-occipital sulcus, POS; calcarine sulcus, CaS. An expanded view of this surface near calcarine is overlaid with a color map showing the response phase at each location for an eccentricity (E) and angle experiment (F) (see the colored legends). The stimuli covered the central 16 degrees radius. Calcarine sulcus contains the V1 hemifield map of the contralateral visual field. For clarity, only locations near the calcarine sulcus are colored, and only locations with a powerful response are shown.

is presented, for example, a series of contrast patterns in concentric rings at different diameters (Figure 3A). The responses to the series of rings are used to estimate the most effective eccentricity. The angular measurements compare the responses to a series of contrast patterns comprising wedges that rotate around the fixation point; the responses from the different angles are interpolated to estimate the most effective angle (Figure 3B). Taken together, the two measurements specify the most effective visual field position in polar coordinates (eccentricity, angle).

A number of experimental decisions influence the quality of the map measurements (see the Discussion in Wandell et al., 2005). When cortical locations within a map are highly responsive to a small region of the visual field, ring and wedge measurements can produce very clear maps. A modern data set measuring the response at a location within V1 to a series of rings yields an fMRI modulation that is 15–20 standard deviations above the noise (Figure 3C). These data show that cortex within human V1 responds powerfully to stimuli in a small range of visual field eccentricities. The most effective visual field eccentricity smoothly changes from more foveal to more peripheral measuring from posterior to anterior calcarine; this defines the V1 eccentricity map (Figures 3D and 3E). Similarly, there is a peaked response as the wedge changes angle, and the most effective angle varies smoothly across a hemifield representation measuring from the superior to inferior lip of the calcarine sulcus (Figure 3F).

The traveling-wave method provides three advantages compared to earlier methods (Fox et al., 1987; Schneider et al., 1993; Shipp et al., 1995). First, the traveling-wave method presents an orderly series of visual field locations from which the most effective location can be interpolated using simple mathematical methods. Second, the entire visual field layout is estimated, and the visual field map

description is not limited by the choice of certain critical visual field locations (e.g., horizontal and vertical meridians). Third, comparing stimuli at certain critical visual field locations with a blank field creates a diffuse cortical response, spreading as much as a centimeter in V1 (Fox et al., 1987). Similarly, alternating nonoverlapping stimuli at specific visual field locations (e.g., horizontal and vertical meridians) may activate neurons whose receptive fields overlap but are not centered on the stimulus (Dumoulin and Wandell, 2007). While these approaches can give a rough estimate of map boundaries, such measurements are not well-suited for the description of a visual field map, for which the identification of the most effective visual field position for each location within a map is key. The traveling-wave method is a differential measurement; for each cortical location, the most effective stimulus is estimated by comparing the responses to a set of stimuli. Such differential measurements are better suited to identifying a variety of maps using neuroimaging methods (Grinvald, 1985).

The traveling wave method is effective for measuring field maps with neurons that have small receptive fields that are mainly confined to one hemifield, such as V1. The visual field maps we summarize in the next several sections were obtained using these methods. However, as we explain later, the traveling-wave method has limitations, particularly when measuring maps with large receptive fields that include the fovea. In the last section of this paper, we describe new developments designed to overcome these limitations.

Identifying Visual Field Maps

In this review, we describe “visual field maps” rather than “visual areas.” Van Essen (2003) explains that a visual area can be identified based on (1) architecture, (2) connectivity, (3) visual topography, or (4) functional characteristics. This definition is fraught with controversy because these empirical criteria may conflict, and reasonable

people can differ on the definition of a visual area (for extended discussions see [Rosa and Tweedale, 2005](#); [Wandell et al., 2005](#)). There are also practical limitations to using these criteria in human cortex. For example, architecture and connectivity are not easily accessible *in vivo*, and we have limited information about these properties in human. Further, identifying areas based upon functional characteristics is important, but we are not close to a satisfactory resolution of this question. Indeed, such a resolution may never occur because of the diversity of neural populations in most areas and the fact that basic response properties can be altered by feedback from other cortical regions; thus, small differences in experimental design and interpretation of the measurements may also lead to differences in area definition. Hence, we emphasize measurements of visual field maps because the idea of the visual field map is relatively straightforward, and it can be made in the living human brain. These maps can then be a basis for the study of architecture, connectivity, and functional characteristics.

Visual field maps are identified by a number of criteria that build on the established layout of early visual field maps V1/2/3 and V3A. These criteria are satisfied by the visual field maps presented in [Figure 2](#). First, by definition, each visual field map contains no more than a single representation for each point in the visual field; that is, two parts of cortex that respond preferentially to the same visual field location must be in distinct visual field maps ([Press et al., 2001](#)).

To be considered as a visual field map, a region of cortex should represent a substantial portion of the visual field, though perhaps not all ([Zeki, 2003](#)). The qualification about visual field coverage arises in part for biological and in part for methodological reasons. Biologically, cortical maps do not represent each visual field region with equal surface area. For example, the V1 visual field map dedicates a larger portion toward the fovea ([Figure 1](#)), and other visual field maps appear to be skewed in other ways (e.g., [Brewer et al., 2005](#); [Ejima et al., 2003](#); [Pitzalis et al., 2006](#)). When a map devotes very little area to a visual field region, functional neuroimaging may not be able to detect the representation. Current functional imaging methods also limit the ability to assess the completeness of the representation. In the eccentricity dimension, foveal regions are poorly distinguished with current methods, and stimulus presentation considerations impose further limits. In the angular dimension, various resolution issues, such as smoothing, optical defocus, and partial-volume effects all limit the precision of estimating the representation at visual field map borders, and interactions between receptive field size and stimuli distort visual field maps ([Dumoulin and Wandell, 2007](#)). Hence, we accept a region as a map if it represents a substantial part of the visual field.

Second, we accept a region as a map if it represents a substantial part of the visual field in an orderly fashion; that is, the visual field map should generally be contiguous in both the eccentricity and angle dimensions - though

a small number of discontinuities are expected. The most obvious discontinuity is the division of the hemifield representation between the two hemispheres. Also, V2 and V3 are further subdivided at the horizontal midline within a hemisphere, so that these visual field maps are separated into four distinct quarterfield representations that are grouped into a single map. Discontinuities are commonly used to define visual field map borders; the absence of a discontinuity is evidence for an integrated map. All of the maps in shown in [Figure 2](#) have a discontinuity in the visual field representation with bordering maps.

Third, the basic features of a visual field map should be consistent across individual subjects, but even well-accepted maps can vary in size (e.g., [Dougherty et al., 2003](#)) and precise anatomical location (e.g., [Dumoulin et al., 2000](#)). Despite these variations, the relative locations and orientations of the visual field maps should form a consistent topological pattern, with adjacency preserved. Consistency of measurements across independent laboratories further strengthens the evidence for a given visual field map. Most of the visual field maps presented in [Figure 2](#) have been confirmed by several independent laboratories, though some have not (i.e., VO-2 and IPS-4).

There are many difficulties in choosing appropriate stimuli or performing the precise measurements needed to identify specific maps. For example, the maps on the ventral surface are clarified by sampling finely in the central visual field, while many dorsal maps and V6 are best revealed using parafoveal or even very large stimuli. Stimulus selection as well as analysis methods can influence the ability to see individual maps. Therefore, multiple reports of the same pattern from different labs should not be outweighed by the occasional inability to identify these maps (see Discussion in [Wandell et al., 2005](#)).

In some cases, visual field map borders can be securely identified manually. In addition, automatic methods have been developed to provide more objectivity and to support quantitative analyses. One automated method computes visual field map signs ([Dumoulin et al., 2003](#); [Serenó et al., 1995](#); [Warrking et al., 2002](#)). An advantage of this method is that it identifies neighboring visual field maps without prior assumptions about the visual field map layout. A disadvantage is that only visual field maps with opposite field signs are distinguished, and this is not always the case. For example, V3A and LO-1 have the same field sign, and the visual field sign method collapses both regions into one large undifferentiated region lateral to V3d. A second automatic method fits a model of the visual field map layout to the data ([Dougherty et al., 2003](#)). The advantage of this method is that it takes into account the full representation of the visual field maps. Furthermore, the fit allows interpolation of specific points in the visual field map which in turn facilitates measurements of visual field map properties, such as surface area and cortical magnification. The disadvantage is that the method needs an a priori model of the visual field layout.

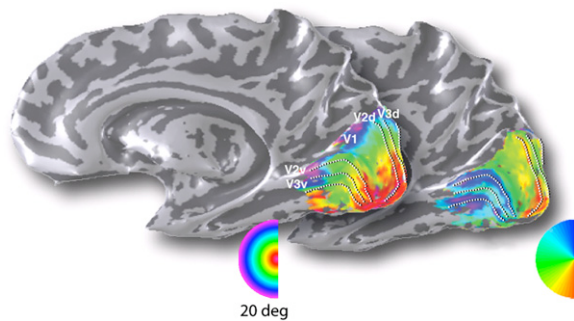


Figure 4. V1, V2, and V3 Visual Field Maps

Visual field maps are measured in the right hemisphere of a single subject using expanding ring and rotating wedge stimuli. The color overlay indicates the eccentricity (left) or angle (right) that produces the most powerful response at each cortical location. The stimuli covered the central 20 degrees radius. For clarity, only responses near the medial occipital cortex are shown. The stimulus-driven responses shown in this paper are substantially above statistical threshold ($p < 0.001$, uncorrected). Other details as in Figure 3.

Human Visual Field Maps

Posterior-Medial Maps: V1, V2, and V3

The traveling-wave fMRI measurements clearly reveal three human hemifield maps near the calcarine sulcus in the occipital lobe (DeYoe et al., 1996; Engel et al., 1997; Sereno et al., 1995; Figure 4). Primary visual cortex (V1), which receives direct input from the retinogeniculate pathway, occupies calcarine cortex and represents a hemifield of visual space. Two additional maps (V2, V3) occupy a strip of cortex, roughly 1–3 cm wide, which encircles V1. V2 and V3 both contain discontinuous hemifield maps, which are divided along the horizontal meridian. This discontinuity creates two quarterfield maps in V2 and V3, each of which has one long edge representing the horizontal meridian and a second representing the vertical meridian.

The eccentricity representations for these three areas run in register. The eccentricity map begins at the large foveal representation on the ventral-lateral surface near the occipital pole, and increasingly peripheral stimuli are represented at increasingly anterior positions along the medial surface. In addition to the parallel eccentricity maps, the vertical meridian representations of V1/V2 are adjacent to one another, as are the horizontal meridian representations of V2/V3.

Apart from the overall scale (macaque V1 is about half the size of human V1) the angular and eccentricity maps in these three maps are quite similar in the two species. Common features include the large confluent foveal representation, the concentric, unified organization of the eccentricity maps across the three areas, and the separation of the V2 and V3 maps into quarterfield representations surrounding V1. In both species there is more cortical surface area allocated to the central than peripheral visual field representation. Complete quantitative formulae defining the relationship between visual field and cortical surface have been developed and analyzed (Balasubra-

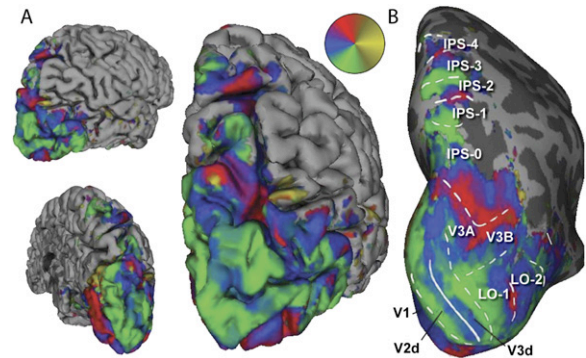


Figure 5. Visual Field Maps on the Dorsal and Lateral Surface of the Human Brain

Adapted from Figure 1 in Swisher et al. (2007) Angular mapping with a rotating wedge stimulus produces modulation of the BOLD signal in a substantial portion of posterior cerebral cortex. The images show the right hemisphere of a single subject. (A) The reconstructed pial surface is shown from posterior lateral (top left), posterior medial (bottom left), and posterior dorsal (right) views. In these views, the cortex is folded as in the normal anatomical state. (B) The value of inflation for visualization is illustrated; notice that the data within the sulci that are occluded in the previous images become visible, and it is much easier to appreciate the reversals in the angular representation that are an important indicator of the boundary between visual field maps (solid and dashed lines). The stimuli covered the central 12 degrees radius.

manian et al., 2002; Schira et al., 2007; Schwartz, 1977). The relationship between cortical position and eccentricity is approximated by a simple exponential function (Dougherty et al., 2003; Engel et al., 1997; Qiu et al., 2006).

There are differing views regarding V3. For example, in macaque, Van Essen and colleagues observed anatomical differences between the dorsal and ventral quarterfield representations surrounding V2. They proposed dividing V3 into two distinct areas, naming the dorsal map V3 and the ventral map VP (Burkhalter et al., 1986), and these terms are used sometimes to identify the dorsal and ventral strips of human V3 (e.g., Pitzalis et al., 2006). Recent anatomical measurements in macaque suggest that the connectivity is similar between macaque V3 and VP, supporting the idea that these two quarterfield maps are part of a single functional entity (Lyon and Kaas, 2002; Wandell et al., 2005; Zeki, 2003). Human fMRI measurements do not offer any definitive support for the hypothesis that the dorsal and ventral maps are fundamentally different; hence, the human maps are most commonly called V3-dorsal and V3-ventral (V3d and V3v).

Dorsal Maps: V3A, V3B, V6, and IPS-X

Several research groups confirm the existence of a collection of visual field maps in dorsal cortex, extending from the anterior portion of V3 into the intraparietal sulcus (IPS) (Figure 5). The map directly adjacent to V3 has many similarities to macaque V3A and is given the same name. A map sharing a confluent fovea with V3A, and now called V3B, was also observed by many groups. More recently, several smaller (400–700 mm²) maps have been identified from the posterior portion of the IPS

to several centimeters anterior (Press et al., 2001; Schluppeck et al., 2005; Sereno et al., 2001; Silver et al., 2005; Tootell et al., 1998). The organization of the human visual field maps beyond V3 and V3A may diverge from the macaque maps, and thus we follow a neutral labeling scheme from the human literature, in which the maps in the IPS are numbered according to their position (Swisher et al., 2007; Wandell et al., 2005).

V3A and V3B. Adjacent to the dorsal quarterfield of V3 (V3d), human cortex contains a hemifield map. The human map borders the anterior portion of V3d and was described in the early human fMRI cortical mapping papers as an angular representation beyond V3 near the transverse occipital sulcus (TOS) (DeYoe et al., 1996; Tootell et al., 1997). This region was called human V3A, because its location is similar to macaque V3A. The angular representation begins at the lower vertical meridian at the border with V3d, spans the horizontal meridian, and then continues into the upper visual field to end at the upper vertical meridian. Notably, V3A only borders V3d in the anterior region that represents the more peripheral visual field.

Dorsal and lateral to V3A, there is another hemifield map, V3B. The V3A and V3B maps share a discrete fovea. This foveal representation is separate and anterior to the confluent fovea of V1/2/3 in the posterior IPS (Figure 5). The eccentricity map near this foveal representation expands concentrically. Thus, the map represents increasingly peripheral locations in the visual field in both lateral and medial directions. Similar to the V1/V2/V3 maps, the angular representations of V3A and V3B partition the confluent eccentricity representation into two discrete maps. The corresponding angular maps of V3A and V3B span both the lateral and medial eccentricity representations: the relatively medial map is V3A, while the relatively lateral map is V3B.

The V3B map has been confirmed by several independent laboratories. Unfortunately, some of the early descriptions in the literature—including from this laboratory—were confusing or inaccurate. These errors have now been corrected in recent papers (Larsson and Heeger, 2006; Swisher et al., 2007), and we repeat the correction here. Smith et al. first described a lower quarterfield map they called V3B (Smith et al., 1998). This map was adjacent to the central representation of dorsal V3. This organization can be seen in Figure 3 in Press et al. (2001), but those authors incorrectly labeled a different map, sharing a foveal representation with V3A, as V3B. In fact, the map they called V3B was a new hemifield map and not the original map proposed by Smith and colleagues. The confusion likely arose from differences in the clarity of the eccentricity measurements near V3A between different labs; Press et al. found a clear, discrete foveal representation for V3A that had been harder to resolve in the earlier measurements of Smith and others. Over time, the V3B label has stuck with the map adjacent to V3A.

Several years later, Larsson and Heeger (2006) measured additional visual field representations on the lateral occipital surface spanning the region of the original map

identified by Smith et al. Larsson and Heeger proposed that we retain the V3B name for the map that shares a confluent fovea with V3A and that we introduce new labels for the two more lateral hemifield maps; the one originally described in part by Smith is called LO-1 (lateral occipital -1), and the new map inferior and adjacent to LO-1 is called LO-2. Swisher et al. (Swisher et al., 2007) followed this notation. We use that terminology here.

V6. Two groups have recently reported a human visual field map located in the parieto-occipital sulcus adjacent to V2, V3, and V3A (Pitzalis et al., 2006; Stenbacka and Vanni, 2007). The representation of the upper visual field is located anterior and medial to V2 and V3, and the lower field representation is medial and slightly anterior to V3 and V3A. V6 contains a distinct foveal representation as well as a large representation of the visual periphery. Its position relative to the surrounding posterior and dorsal maps and the fact that the human map appears to represent mainly peripheral stimuli suggest that it is homologous to macaque V6 (Galletti et al., 1996, 1999).

IPS-0 (V7). Tootell et al. (1998) described a map located immediately anterior to V3A that they named V7. This map begins with a representation of the upper vertical meridian at the border of V3A, spans at least a hemifield of visual space (Press et al., 2001), and contains a second dorsal foveal representation distinct from that of V3A/V3B. This region may be in the same location as macaque area DP, but there is no evidence yet for a homology between these regions. Measurements of spatial attention by Tootell et al. (1998) showed an increase in MR signal within V7 when attention was directed to the same retinotopic location as a visual stimulus. V7 lies within the IPS and shares a confluent fovea with another hemifield map along the IPS, IPS-1, suggesting that the two maps form a cluster. Therefore, Swisher et al. (2007) proposed renaming V7 as IPS-0. We follow the IPS-0 nomenclature because it better describes the anatomical position of this visual field map.

IPS-1/2/3/4. Several maps along the intra-parietal sulcus (IPS), anterior to IPS-0, have now been described. Sereno et al. (2001) identified a map many centimeters anterior to IPS-0, using an eye-movement memory task. They write that it is “unlikely that our large parietal activations were due to passive sensory responses,” and they speculate that this map is a homolog of macaque lateral intra-parietal area (LIP). Using a variety of techniques, including eye movements and attentional modulations, Silver et al. (2005) and Schluppeck et al. (2005) identified two visual field maps anterior to IPS-0. The first of these, IPS-1, shares a confluent fovea with IPS-0 and appears to form a cluster (Swisher et al., 2007). The second, IPS-2, can be identified from a reversal in the angle map and is further anterior. They show that IPS-1 and IPS-2 can be identified both using saccades and with attention shifts. Schluppeck et al. (2005) point out that these maps are posterior to the map reported by Sereno et al. (2001) using the delayed-saccade task.

Two groups confirm the location and properties of the IPS-1/2 maps (Hagler et al., 2007; Swisher et al., 2007).

In addition, Swisher et al. (2007) showed that these maps could be identified using sensory stimulation without a saccadic or attentional manipulation. Moreover, they describe two visual field maps anterior to IPS-2, which they labeled IPS-3 and IPS-4. It seems likely that IPS-3 corresponds to the map called the putative homolog of monkey LIP by Sereno et al. (Hagler et al., 2007; Sereno et al., 2001).

Lateral Maps: LO-1, LO-2, and hMT

LO-1, LO-2. Responses to traveling-wave stimuli in lateral occipital (LO) cortex, a region extending laterally and anteriorly from dorsal V3, differ substantially from responses in primary visual cortex. We attribute this to a difference in receptive field size (about 5x) between neurons in V1 and LO cortex (Dumoulin and Wandell, 2007). Conventional traveling-wave methods are not well-suited to uncovering visual field maps under these conditions, and several early measurements using the traveling-wave method reported no compelling retinotopy (Grill-Spector et al., 1998; Malach et al., 1995; Tootell and Hadjikhani, 2001).

The naming conventions associated with LO cortex have undergone several transformations. Investigators measuring object and face recognition first observed modulations that spanned lateral occipital and ventral occipital-temporal cortex. They named the entire functionally defined zone as the lateral occipital complex (LOC), with additional functional subdivisions (Grill-Spector et al., 1999; Grill-Spector and Malach, 2004; Malach et al., 1995). In search for a map to match a proposed ventral V4 quarterfield map, Tootell and Hadjikhani (2001) call this region “anterior to V3A, posterior to MT+, and superior to ventral V4” the V4d-topo (for “dorsal V4 topologue”) to represent the likely anatomical region where they expected to find a human V4 map homologous to macaque dorsal V4. Across this region, they measured crude retinotopic eccentricity responses and proposed dividing LO into two regions representing the central (LOc) and peripheral (LOp) visual field. Subsequently, Tyler et al. (2005) measured a lower field representation in the region between V3A, V3d, and hMT+ which they called dorsolateral occipital (DLO).

Recent compelling reports now identify two clear hemifield maps adjacent to the central representation of V3 on the lateral occipital surface (Figure 6; see also Figure 5) (Larsson and Heeger, 2006; Swisher et al., 2007). These maps represent the contralateral visual hemifield, and they have a foveal representation that is confluent with that of V1, V2, V3, and hV4. The angle representation in LO-1 is the mirror of V3, and that in LO-2 is the mirror of LO-1. In both cases, the representation at the boundary is at the upper (V3/LO-1) or lower (LO-1/LO-2) vertical meridian. The visual field eccentricity representations in LO-1 and LO-2 are parallel. Currently, it is not clear whether there is a gap between the relatively anterior map (LO-2) and hMT+.

The notation LO-X seems appropriate for visual field maps in lateral occipital cortex, as it is consistent with the nomenclature for the ventral (VO-X) and dorsal (IPS-

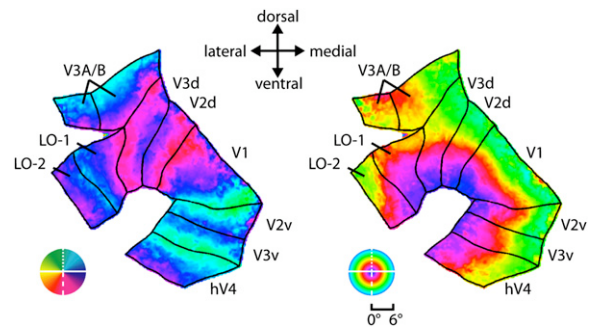


Figure 6. Visual Field Maps Illustrated on a Computationally Flattened Cortical Representation

Adapted from Figure 1 in Larsson and Heeger (2006). A flattened representation of cortex illustrates the spatial relationship between maps near the occipital pole in the left hemisphere. The maps show the angular (left) and eccentricity (right) maps averaged across 15 hemispheres. In the left column, color indicates polar angle (inset legend). In the right column, color indicates eccentricity between 0° and 6° (inset legend).

X) maps, and homology to macaque areas is unclear (Larsson and Heeger, 2006; Swisher et al., 2007; Wandell et al., 2005). Based on retinotopic responses seen in our data and that from other laboratories, we suspect that over time the entire LOC and other regions on the ventral and lateral surface will be subdivided into visual field maps. Should this occur, the LO Complex may be further subdivided into visual field maps. We propose that these be identified as either LO-X or VO-X, according to their anatomical location.

hMT+. The human homolog of macaque MT (also referred to as V5) is found within a highly motion-sensitive region on the border between lateral occipital and temporal cortex (Dumoulin et al., 2000; Tootell et al., 1995; Watson et al., 1993). The functional definition of this region probably includes several visual field maps in addition to hMT (e.g., MST). To acknowledge the imprecision in the identification, the region defined by motion responsivity is referred to as hMT+ (DeYoe et al., 1996).

The initial definition of MT was based on a visual field map (Allman and Kaas, 1971). Hence, there is a strong presumption that one should be able to identify a specific human MT map. Several attempts have been made to subdivide the region hMT+ using visual field maps and other functional measurements. There is a particular focus on separating hMT from an adjacent area identified in monkey, MST (Beauchamp et al., 2007; Dukelow et al., 2001; Goossens et al., 2006; Huk et al., 2002; Smith et al., 2006). Huk et al. (2002) reported the existence of a visual field map within the region hMT+, and they proposed that this visual field map is hMT. The small size of the MT visual field map and the variability of map position across individuals have made this region difficult to study. While the presence of at least one visual field map is certain, multiple small maps are likely to exist in this region. The literature contains several images that show suggestive maps in the hMT+ region, and we suspect that with

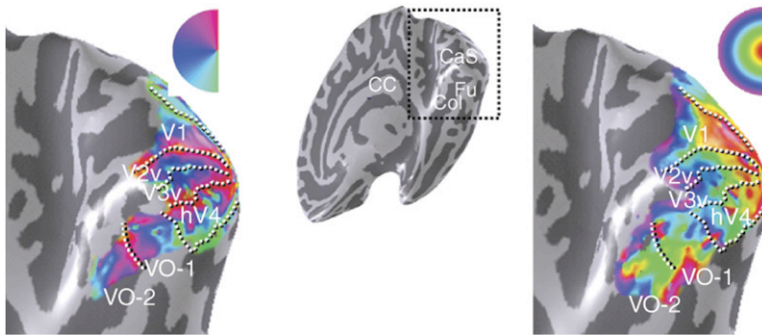


Figure 7. Visual Field Maps on the Ventral Occipital-Temporal Surface of the Human Brain

The ventral occipital region of interest in the right hemisphere of a single subject is shown in the center inset (Fu, fusiform gyrus; Col, collateral sulcus; CaS, calcarine sulcus). Angle (left) and eccentricity (right) measurements were made using a 3 degree radius stimulus. Dashed lines indicate the estimated boundaries between several visual field maps, including the ventral portions of V1, V2, and V3 as well as hV4, VO-1, and VO-2. For clarity, only responses within these visual field maps are colored, and only locations with a powerful response are shown. Other details as in Figure 3.

improvements in technology these maps will be clarified in the next several years.

Ventral Maps: hV4, VO-1, VO-2

The organization of ventral cortex has been of particular interest because its circuits are essential for seeing objects and color (Zeki, 1993). At first, it was thought the region anterior to ventral V3 was not retinotopically organized (Halgren et al., 1999). But over the years, several investigators found retinotopic responses on the ventral surface (Brewer et al., 2005; Hadjikhani et al., 1998; Kastner et al., 2001; McKeefry and Zeki, 1997; Wade et al., 2002; Wandell et al., 2005).

Several features of the ventral data anterior to V3v, particularly a displaced foveal representation and an angular map exceeding a quarterfield, have been described consistently (Brewer et al., 2005; Hadjikhani et al., 1998; Tyler et al., 2005; Wade et al., 2002). Other aspects of the data are inconsistent across labs, and several models of the ventral maps have been proposed. These include the original V4v/V8 model (Hadjikhani et al., 1998), a grouping developed by Tyler et al. (2005), the hV4/VO model described here (Brewer et al., 2005), and a truncated ventral V4 suggested by Hansen et al. (2007). The traveling-wave method—with its limited ability to measure large receptive fields that span the fovea—will require improvements and modifications to clarify these ventral maps.

hV4. Directly abutting the ventral portion of V3 is a hemifield map, which shares a common eccentricity orientation with the confluent foveal representation of V1/V2/V3 (Figure 7; see also Figure 6) (Brewer et al., 2005). The name hV4 was chosen because part of the map had been named V4(v) by other investigators; the “h” for “human” was added to clarify that the difference between the hV4 map and macaque V4 appears substantial (Brewer et al., 2002, 2005), and the homology between hV4 and macaque V4 remains unproven.

The hV4 eccentricity representation parallels that of V1/V2/V3, but hV4 appears shorter than V3 (Tyler et al., 2005), and its cortical magnification differs quantitatively (Ejima et al., 2003). The angular map in hV4 runs from the upper vertical meridian at the border of V3v across the lateral bank of the collateral sulcus to the lower vertical meridian on the posterior fusiform gyrus. Several independent laboratories have reported measurements adjacent to ventral

V3 consistent with an hV4 map that represents more than a quarterfield of visual space (Brewer et al., 2005; Gardner et al., 2005; Hansen et al., 2007; Larsson and Heeger, 2006; Merabet et al., 2007; Montaser-Kouhsari et al., 2007; Swisher et al., 2007; Tyler et al., 2005; Wade et al., 2002), in contrast to the initial V4v/V8 model which depends upon a quarterfield V4v map.

Hansen et al. (2007) describe a model to reconcile the hemifield hV4 map with macaque V4. They note that macaque V4 surrounds V3, and the dorsal and ventral representations divide slightly below the horizontal meridian (Gattass et al., 1988). They suggest that the ventral region near hV4 represents a larger range of angular values than ventral V4 in macaque, but still falls short of a complete hemifield. They propose a portion of the LO-1 map should be grouped with hV4, completing the representation. According to this scheme, the dorsal V4 strip directly abuts LO-1 with no field reversal. This proposal faces two challenges. First, three independent labs show continuous LO-1 angular maps directly adjacent to V3d with no intervening discontinuity (Larsson and Heeger, 2006; Figure 3 in Press et al., 2001; Swisher et al., 2007). A boundary without a discontinuity is a departure from any other map boundary definition. Second, angular responses near the vertical midline are often difficult to measure because of technical limitations, and these limitations become particularly severe as receptive field size increases, as in hV4. Demonstrating that the angular signals are absent in the brain, and not just missed by the methods, will require further analyses.

VO-1, VO-2. In ventral occipital cortex (VO), two hemifield maps, VO-1 and VO-2, have been described anterior to hV4 (Brewer et al., 2005; Larsson et al., 2006; Liu and Wandell, 2005). The VO-1 and VO-2 eccentricity maps begin in a large distinct foveal representation. The VO-1 lower vertical meridian representation abuts the peripheral representation of hV4 and extends to the peripheral representation of V3v (Larsson et al., 2006). VO-1 and VO-2 share an upper vertical meridian representation. Like the V3A/V3B maps, the eccentricity representation forms a semicircular pattern. The eccentricity map becomes increasingly peripheral as it extends medially across the collateral sulcus and approaches the peripheral representation of V3v.

These ventral maps respond powerfully to central visual stimuli throughout their extent, consistent with the high cortical magnification described in human and macaque ventral cortex (Baizer et al., 1991; Ejima et al., 2003). Increasing the stimulus radius from 3 to 16 degrees expands the responding surface area of V1 considerably along the calcarine sulcus, but the hV4, VO-1 and VO-2 maps expand very little or not at all. Like V1, the surface area of these maps varies across subjects.

We observed traveling-wave responses in many subjects anterior to the VO cluster (Brewer et al., 2005; Wade et al., 2002). These regions have not yet been organized into definitive maps beyond identifying another foveal representation (Wandell et al., 2006). We suspect that this foveal representation indicates the presence of another visual field map cluster, and we propose to term this putative cluster ventral-temporal (VT), with corresponding visual field maps termed VT-1 and so forth.

New Frontiers

Integration with Other Cortical Functions

Visual information must be combined with motor, memory, and other important cortical functions. There are several recent reports showing that visual field maps may be useful in analyzing cortical responses that integrate cortical functions.

Two groups report topographically organized responses in frontal cortex (Hagler et al., 2007; Hagler and Sereno, 2006; Kastner et al., 2007). Although these regions are driven less by stimulus contrast than memory-guided spatial representations, the principle of topography extends beyond sensory maps to related cognitive representations of space.

There are also reports that responses in visual cortex are organized with respect to a visual frame within the scene (d'Avossa et al., 2007; Goossens et al., 2006; McKyton and Zohary, 2007). Such neural representations of visual space are called *spatiotopic* maps. The transformation of retinotopic to spatiotopic maps may be an essential component of integrating visual and motor information. These are important claims, and many laboratories are sure to follow-up these reports. The maps described in this review are thought to be retinotopic, not spatiotopic. It may be, however, that responses in retinotopic maps can be influenced by eye position (DeSouza et al., 2002; McKyton and Zohary, 2007).

Integration with Other Measurement Methods

The visual area concept has been powerful because it forces the scientist to confront several types of information (Van Essen, 2003). In this review, we focus on the visual field maps because information from the human brain about maps has accrued more rapidly and completely than other types of information used in the definition of a visual area. New architectonic information in human is now appearing, and this information will be coordinated with fMRI measurements of human visual field maps (Bridge and Clare, 2006; Eickhoff et al., 2005; Rottschy et al., 2007). Preliminary analysis reveals a good correspon-

dence between functionally and anatomically derived estimates of early visual field maps (Bridge et al., 2005; Wohlschlagel et al., 2005) and hMT+ (Annese et al., 2005; Tootell and Taylor, 1995; Wilms et al., 2005). Additional information about cortical connections is also becoming available through the development of diffusion-weighted imaging (Conturo et al., 1999; Dougherty et al., 2005; Wakana et al., 2004).

Information Integration

There is significant variability in the size and anatomical position of visual field maps between subjects, and there have been several efforts to quantify the variation in size of primary visual cortex. All groups agree that the surface area of V1 commonly varies by a factor as large as 2.5 even among individuals with normal visual function (Amunts et al., 2000; Dougherty et al., 2003; Stensaas et al., 1974), and these variations appear to correlate with other anatomical structures (Andrews et al., 1997). Despite some local variation, there is much regularity in the position and properties of these maps. Van Essen and his colleagues worked to create an atlas that summarizes the key map features (Van Essen, 2005). This ongoing project contains valuable information for scientists seeking to understand the visual pathways and for clinicians looking for general guidance about organization and function.

Monkey and Human Visual Field Maps

The comparison with nonhuman primates is an important source of insight for human cortical organization. Current efforts to map human cortex have diverged; some efforts are guided by nonhuman primate data (e.g., Pitzalis et al., 2006); others have loosened these ties and focus more on the human data at hand (e.g., Brewer et al., 2005; Larsson and Heeger, 2006; Swisher et al., 2007). The visual field mapping discipline profits from both approaches, and it is possible to use fMRI to measure maps in both species (Brewer et al., 2002; Fize et al., 2003). There are limitations to the methods, however, because of the difficulty in controlling eye position and attention in monkey. Using anesthesia and fixed eye position reduces the signal in extrastriate cortex (Brewer et al., 2002); using awake-fixating animals requires training and careful eye-movement tracking (Fize et al., 2003).

The number of neurons in human visual cortex exceeds that of monkey visual cortex. This difference cannot be attributed to the sampling resolution of the visual world but likely reflects the increased visual processing required by cognitive demands that are absent in monkeys, e.g., language and reading (Wandell et al., 2007). These differences in visual cortex size and function would suggest that at least some features in human visual cortex are not present in monkey. As increasing amounts of human visual cortex are explored, the nonhuman primate data offers a less secure model, and homologies between maps are uncertain (Rosa and Tweeddale, 2005).

One important and interesting challenge comes from comparing the V3 and V3A maps in human and macaque. The map topographies are similar in the two species, but the stimulus sensitivities differ: V3A is not responsive to

motion in macaque, but it is strongly responsive in humans (Tootell et al., 1997; Vanduffel et al., 2001). Hence, these areas appear to have homologous maps, but nonhomologous functional properties.

The early studies of human visual field maps use nomenclature established in nonhuman primate studies, i.e., Vx (DeYoe et al., 1996; Dumoulin et al., 2000; Engel et al., 1997; Huk et al., 2002; Schneider et al., 1993; Sereno et al., 1995; Tootell et al., 1995; Watson et al., 1993; Zeki et al., 1991). As our confidence in homology declines, we can err by failing to label two homologous areas the same or by inappropriately labeling two nonhomologous areas the same. As Rosa and Tweedale (2005) observe, giving the same label to nonhomologous areas is more problematic.

We proposed a conservative visual field map nomenclature in human that is derived from the map's human anatomical location and a number, i.e., VO-1/2, LO-1/2, and IPS-0/1/2/3/4 (Wandell et al., 2005). This nomenclature separates efforts to describe visual field map layouts from efforts to establish homologies. Other naming schemes are based on anatomy alone (e.g., dorsal-lateral-occipital, DLO [Tyler et al., 2005]) and/or proposed function (e.g., kinetic occipital, KO [Orban et al., 1995]; or ventral occipital foveal, VOF [Tyler et al., 2005]). We prefer the anatomy-number scheme to nomenclature based on anatomy alone because both the terminology of gross anatomical structures and the anatomical-functional relationships lack the precision to define several small maps in the same region. We support Smith et al. (1998), who oppose naming based upon assumed functional properties because much more extensive studies are required to appreciate fully all the functions of a given visual field map.

The Organization of Visual Field Maps

Several authors have tried to develop hypotheses describing the overall functional and structural organization of visual field maps. These ideas are not very precise, nor are they mutually exclusive. We think that efforts to understand the organization of visual cortex and these maps are important, and so we review several suggestions here.

Two hypotheses about the organization of visual field maps have been particularly influential (Figure 8A). Ungerleider and Mishkin (1982) noted that projections from V1 are carried via two major white matter pathways toward ventral and dorsal extrastriate cortex. They further marshaled evidence showing that ventral occipitotemporal lesions produce visual discrimination deficits, while dorsal occipitoparietal lesions produce spatial deficits, as in a landmark task, without degrading object discrimination. Ungerleider and Mishkin (1982) hypothesized that the ventral pathway is specialized for "identifying *what* an object is" and the dorsal pathway is specialized for "locating *where* an object is" (Figure 8A). The ventral and dorsal pathways are dominated by central and peripheral signals, respectively (Baizer et al., 1991). Milner and Goodale (Goodale and Milner, 1992; Milner and Goodale, 2006) supported the concept of two major functional subdivisions of visual cortex, but they reinterpreted the data

and suggested that the streams have different functional objectives. A rough summary of their view is that the ventral stream represents vision for perception, while the dorsal stream represents vision in service of action.

The principle that the visual pathways comprise two (or more) functional systems is an important part of visual neuroscience theory. The Duplex theory of rod and cone vision is perhaps the best known example; the multiple pathway hypothesis based on a collection of retinal outputs with distinct central targets is yet another important example (Schneider, 1969; Trevarthen, 1968; Wandell, 1995). The idea that cortical maps represent individual functional specializations (Zeki, 1990) or that groups of maps are organized to perform specialized functions is a natural extension of this basic neuroscience principle.

A second important organization was developed by Van Essen and colleagues (Figure 8B). They introduced an anatomical method for developing a hierarchical graph that captures the relationship between visual areas (Felleman and Van Essen, 1991; Van Essen and Maunsell, 1983). The relationships between visual areas in macaque were summarized in a table that classified the connections between areas as ascending, lateral, and descending. The classification was based on the laminar distribution of the connections between areas. They showed how the classification of the connections could be organized into a hierarchical graph beginning in "lower tier" areas, including the LGN and V1, and continuing to "higher tier," such as TEO (Figure 8B). The same data set was analyzed by Young (1992), who used multidimensional scaling to create a nonhierarchical visualization of these data.

Van Essen and colleagues built the hierarchical model as a working summary that could be changed as additional information was accumulated; they were aware that their very large data set contained some substantial uncertainties. There are a number of new developments, such as much new knowledge about the significance of the laminar distribution of projections (Barbas and Rempel-Clower, 1997; Pandya et al., 1988) and the identification of pathways from the LGN to V5 (Bourne and Rosa, 2003; Sincich et al., 2004) that might be incorporated. Also, the question of how subcortical areas fit within the hierarchy, including the whole of the thalamus, is important and under active exploration (Sherman and Guillery, 2001).

Finally, we note two recent proposals about the organization of human visual field maps. Malach and colleagues (Hasson et al., 2002, 2003; Levy et al., 2001) describe "a new organizing principle in which object representations are arranged according to a central versus peripheral visual field bias" (Levy et al., 2001). They suggest that the precise lower-tier visual field maps (V1, V2, and V3) are replaced in more anterior visual cortex by much cruder, or absent, maps that are organized around representations of perceptual entities, including faces, places, and objects. They suggest that major features, such as the angle representation, are absent; the maps retain only an eccentricity bias that is influenced by the retinal image size of the

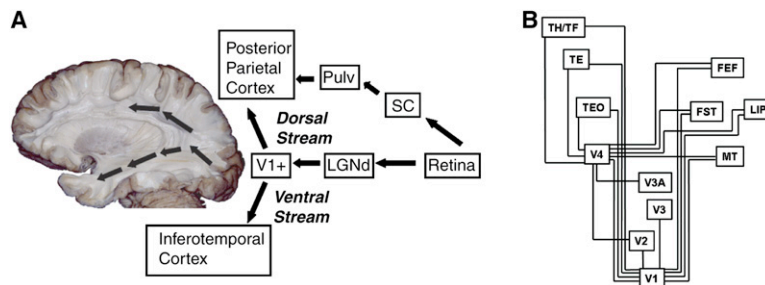


Figure 8. Theories of Visual Field Map Organization

(A) Signals in V1 and nearby maps are essential for vision; damage to these maps causes a visual blindspot (scotoma). Ungerleider and Mishkin (1982) suggest that visual signals enter two large white matter tracts (the superior and inferior longitudinal fasciculus) that are specialized for distinct visual functions. Damage in the projection zones of these tracts does not cause complete blindness but rather specific and dissociable performance deficits. Signals along the superior path appear to be specialized for action or spatial orientation; sig-

nals along the inferior path appear to be specialized for object recognition (Milner and Goodale, 2006; Ungerleider and Mishkin, 1982). (Brain image courtesy of Dr. Ugur Ture.)

(B) Signals between visual field maps are carried along pathways whose axons terminate in distinct patterns. These termination patterns are classified into ascending, descending, and lateral connectivity and establish a hierarchical representation (Felleman and Van Essen, 1991; Van Essen and Maunsell, 1983). A simplified version of the hierarchy, showing the relationship between a subset of the maps in macaque, is shown here. This figure is from Figure 11 in Barone et al. (2000).

object represented by the area. This “eccentricity-bias” model is further reviewed in (Figure 12 in Grill-Spector and Malach, 2004).

Improvements in measurements have revealed more visual field maps in lateral occipital cortex than Malach and colleagues anticipated when framing their hypothesis. In view of these developments, Wandell et al. (2005) suggested an alternative organization (Figure 9). Specifically, they propose that maps are organized into several clusters. A cluster is a group of maps with parallel eccentricity representations; different clusters have distinct eccentricity maps. Within a cluster, the maps can be identified by reversals in the visual field map angle representation. The maps near V1 are the prototypical cluster, but several other clusters—such as near V3A/V3B, IPS, hMT+, and VO—have also been identified (Brewer et al., 2005; Larsen and Heeger, 2006; Schluppeck et al., 2005; Silver et al., 2005; Swisher et al., 2007; Wandell et al., 2006).

Improving Visual Field Map Measurements

The traveling-wave methods successfully identified many visual field maps, but the methods have significant limitations. First, these stimuli are poorly designed to measure neuronal populations whose receptive fields are centered on the fovea (Dumoulin and Wandell, 2007; Figure 7 in Press et al., 2001). A neuron whose receptive field is centered on the fixation point will not modulate its response to a wedge. This limitation is crucial because the fovea is in many cases the most important component of the perceptual representation. Consequently, visual field maps near the central field representation are not easily measured; these regions are commonly referred to as the foveal confluence (e.g., Schira et al., 2007).

Second, traveling-wave estimates of the eccentricity map using expanding rings are nonlinearly distorted, again most prominently when cortical response regions overlap with the fovea (Dumoulin and Wandell, 2007).

Third, the traveling wave method fails when neuronal receptive fields are large (Dumoulin and Wandell, 2007). The traveling-wave method—or even a method that contrasts horizontal and vertical meridians—will treat these regions as nonresponsive or weakly response cortex. To detect

the fact that cortex responds to all stimuli, it is necessary to include a blank control.

In the last several years new methods have emerged that may improve the ability to measure the visual field maps in visual cortex. These methods also promise to identify additional information about the neurons within the map.

Alternative Stimulus Sequence

Several groups proposed using temporally orthogonal stimulus sets to measure visual field maps (Buracas and Boynton, 2002; Hansen et al., 2004; Vanni et al., 2005). Rather than systematically sweeping out the eccentricity or angle, these methods create a series of patches derived from rings and wedges. These images are constructed in such a way that each of the patches has its own, unique temporal sequence. Such temporal stimulus sequences are used commonly in multifocal EEG/MEG measurements, and there are a variety of ways of constructing the orthogonal sequences. One approach is to use the M-sequence method developed by Sutter and Tran (1992). The data are analyzed using a general linear model (GLM) to derive how effectively each stimulus patch contributes to the response at each cortical location. Within V1, the simple linear model approach accurately identifies the visual field position that most effectively stimulates each cortical location; this produces a visual field map.

This method has several theoretical advantages. First, it includes a blank stimulus, making it possible to assess whether all the stimuli are equally effective. Second, the method avoids the difficulties seen in ring and wedge stimuli when neuronal receptive fields span the fovea, because the stimuli comprise spatially localized patches. Third, the method allows a description of the population receptive field (Yoshor et al., 2007). The method depends significantly on the assumption that the BOLD response is linear across space, which appears to be a good approximation for signals in V1 (Hansen et al., 2004). Whether spatial linearity is satisfied in other extrastriate regions remains to be tested. At present, however, there are no regions where M-sequences uncover maps that are missed by conventional traveling-wave methods, and the theoretical advantages remain to be demonstrated empirically.

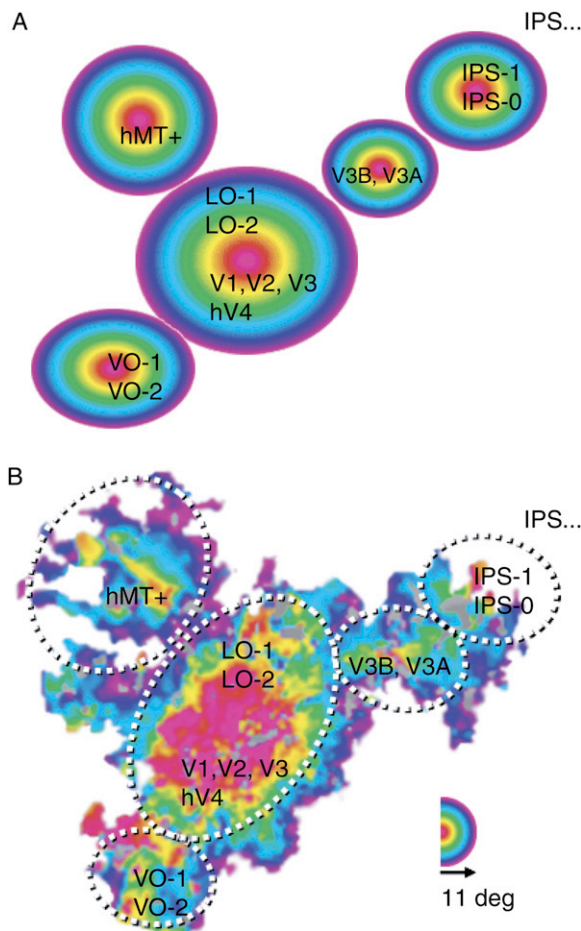


Figure 9. Visual Field Map Clusters

(A) A schematic diagram of the organization of eccentricity representations in visual cortex is shown. The image shows the visual field map grouped into clusters, as they would appear on flattened cortex. The concentric colored circles designate the eccentricity representations of maps within a cluster. Each cluster contains several visual field maps that can be delineated based on the angle maps.

(B) Eccentricity measurements spanning 0° – 11° are shown on a flattened section of cortex from the left hemisphere of a single subject. Dotted lines overlaid on the flattened data illustrate the clusters. Color legend (inset) shows the eccentricity that most effectively drives each cortical location. The bottom image is cropped to show only the data within defined visual field maps. IPS-2/3/4 were not measured in this data set.

Model-Based Analysis of the Time Series

As the alternative name (phase-encoded retinotopic mapping) for the traveling-wave method implies, the method does not interpret all the information in the time series. Rather, the method uses the phase of the time-series modulation to find the most effective visual field position. From the earliest papers, however, investigators were aware that the time series contains additional information. For example, Tootell et al. (1997) noticed that V1 and V3A responses to the same stimulus differed; they interpreted these as reflecting differences in the receptive field size of neurons in these maps. Other investigators used addi-

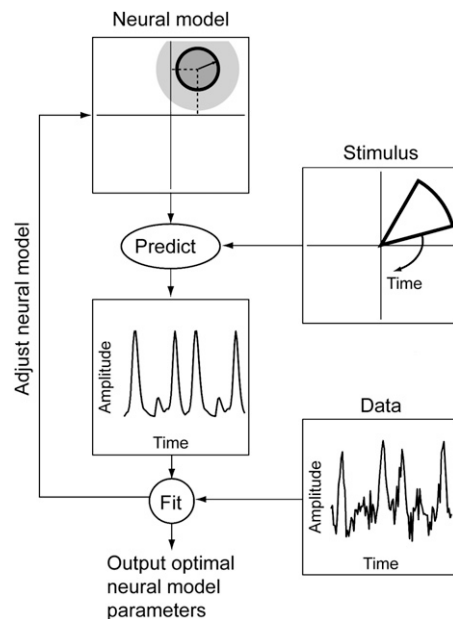


Figure 10. Computational Models to Estimate the Neural Responses Driving the BOLD Signal

Adapted from Figure 2 in Dumoulin and Wandell (2007). The neural model describes certain neural properties, such as receptive field center, size and scatter, along with a model of nuisance factors, such as the hemodynamic response, eye movements, and so forth. Several of these nuisance factors can be estimated, thereby sharpening our estimates of the neuronal properties. The neural model is combined with the stimulus to generate the prediction. The neuronal model parameters are adjusted for each cortical location to minimize the difference between the prediction and the data. As the solution converges, the neural model parameters are output for analysis.

tional measures of the time series (duty cycle) to identify differences between neural populations in different maps or between portions of the maps representing the central and peripheral visual field (Larsson et al., 2006; Li et al., 2007; Smith et al., 2001).

Thirion et al. (2006) developed an analysis to use all the time-series information to decode the visual stimulus in the occipital lobe. The stimulus reconstruction was performed using two different algorithms, one from an explicit forward model based upon the traveling wave paradigm and a second implicit reconstruction based on data classification techniques. Both algorithms predicted the stimulus with significant accuracy. However, the implicit data classification techniques performed better, which Thirion et al. attributed to shortcomings of the time-series analysis by the traveling wave method.

The trend toward using more time-series information is continuing. Dumoulin and Wandell recently developed methods for using the fMRI time series to model neuronal populations (Figure 10) (Dumoulin and Wandell, 2007). Specifically, they compute a model of the population receptive field (pRF) from responses to a wide range of stimuli and produce estimates of the visual field map as well as other neuronal population properties, such as the population receptive field size and the ipsilateral extent of the

population receptive fields (laterality). This method decouples the visual field map measurements from the rings and wedges, thus eliminating some of the difficulties with the conventional traveling-wave approach. They show that visual field maps obtained with the pRF method are more accurate than those obtained using conventional visual field mapping, and they delineate the visual field maps to the center of the foveal representation. The pRF method extracts additional information beyond the maps and generalizes both the traveling wave method and alternative stimulus sequence techniques.

Conclusions

During the past 15 years, functional MRI has produced a wealth of data about human visual field maps. We are not at the end of the process: improvements in MR instrumentation, as well as new analytical methods, promise to yield more insight into these functional structures. Further, new advances in MR and computational methods, such as diffusion-weighted imaging coupled with tractography, MR-spectroscopy, and MR-relaxometry, will provide more precise information about the molecular and cellular organization of visual cortex. These advances are certain to provide important tools for answering questions about human visual functions, including development, plasticity, and perceptual function.

ACKNOWLEDGMENTS

The second and third authors contributed equally to this work. This work was supported by National Eye Institute Grant RO1 EY03164 (BW) and Larry L. Hillblom Foundation fellowship 2005/2BB to SD. We thank D. Heeger, J. Swisher, J. Larsson, and five anonymous reviewers for their comments on the manuscript.

REFERENCES

Allman, J.M., and Kaas, J.H. (1971). A representation of the visual field in the caudal third of the middle temporal gyrus of the owl monkey. *Brain Res.* 31, 85–105.

Amunts, K., Malikovic, A., Mohlberg, H., Schormann, T., and Zilles, K. (2000). Brodmann's areas 17 and 18 brought into stereotaxic space-where and how variable? *Neuroimage* 11, 66–84.

Andrews, T.J., Halpern, S.D., and Purves, D. (1997). Correlated size variations in human visual cortex, lateral geniculate nucleus, and optic tract. *J. Neurosci.* 17, 2859–2868.

Annese, J., Gazzaniga, M.S., and Toga, A.W. (2005). Localization of the human cortical visual area MT based on computer aided histological analysis. *Cereb. Cortex* 15, 1044–1053.

Baizer, J.S., Ungerleider, L.G., and Desimone, R. (1991). Organization of visual inputs to the inferior temporal and posterior parietal cortex in macaques. *J. Neurosci.* 11, 168–190.

Balasubramanian, M., Polimeni, J., and Schwartz, E.L. (2002). The V1 -V2-V3 complex: Quasiconformal dipole maps in primate striate and extra-striate cortex. *Neural Netw.* 15, 1157–1163.

Barbas, H., and Rempel-Clower, N. (1997). Cortical structure predicts the pattern of corticocortical connections. *Cereb. Cortex* 7, 635–646.

Barnes, G.R., Hess, R.F., Dumoulin, S.O., Achtman, R.L., and Pike, G.B. (2001). The cortical deficit in humans with strabismic amblyopia. *J. Physiol.* 533, 281–297.

Barone, P., Batardiere, A., Knoblauch, K., and Kennedy, H. (2000). Laminar distribution of neurons in extrastriate areas projecting to visual areas V1 and V4 correlates with the hierarchical rank and indicates the operation of a distance rule. *J. Neurosci.* 20, 3263–3281.

Baseler, H.A., Brewer, A.A., Sharpe, L.T., Morland, A.B., Jagle, H., and Wandell, B.A. (2002). Reorganization of human cortical maps caused by inherited photoreceptor abnormalities. *Nat. Neurosci.* 5, 364–370.

Baseler, H.A., Morland, A.B., and Wandell, B.A. (1999). Topographic organization of human visual areas in the absence of input from primary cortex. *J. Neurosci.* 19, 2619–2627.

Beauchamp, M.S., Yasar, N.E., Kishan, N., and Ro, T. (2007). Human MST but not MT responds to tactile stimulation. *J. Neurosci.* 27, 8261–8267.

Blinkov, S., and Glezer, I. (1968). *The Human Brain in Figures and Tables* (New York: Plenum).

Bourne, J.A., and Rosa, M.G. (2003). Neurofilament protein expression in the geniculostriate pathway of a New World monkey (*Callithrix jacchus*). *Exp. Brain Res.* 150, 19–24.

Braitenberg, V., and Schüz, A. (1998). *Cortex: Statistics and Geometry of Neuronal Connectivity*, Second Edition (Heidelberg, Germany: Springer Verlag).

Brewer, A.A., Liu, J., Wade, A.R., and Wandell, B.A. (2005). Visual field maps and stimulus selectivity in human ventral occipital cortex. *Nat. Neurosci.* 8, 1102–1109.

Brewer, A.A., Press, W.A., Logothetis, N.K., and Wandell, B.A. (2002). Visual areas in macaque cortex measured using functional magnetic resonance imaging. *J. Neurosci.* 22, 10416–10426.

Bridge, H., and Clare, S. (2006). High-resolution MRI: In vivo histology? *Philos. Trans. R. Soc. Lond. B Biol. Sci.* 367, 137–146.

Bridge, H., Clare, S., Jenkinson, M., Jezzard, P., Parker, A.J., and Matthews, P.M. (2005). Independent anatomical and functional measures of the V1/V2 boundary in human visual cortex. *J. Vis.* 5, 93–102.

Brindley, G.S., and Lewin, W.S. (1968). The sensations produced by electrical stimulation of the visual cortex. *J. Physiol.* 196, 479–493.

Buracas, G.T., and Boynton, G.M. (2002). Efficient design of event-related fMRI experiments using M-sequences. *Neuroimage* 16, 801–813.

Burkhalter, A., Felleman, D.J., Newsome, W.T., and Essen, D.C.V. (1986). Anatomical and physiological asymmetries related to visual areas {V3} and {VP} in macaque extrastriate cortex. *Vision Res.* 26, 63–80.

Collins, D.L., Neelin, P., Peters, T.M., and Evans, A.C. (1994). Automatic 3D intersubject registration of MR volumetric data in standardized Talairach space. *J. Comput. Assist. Tomogr.* 18, 192–205.

Conturo, T.E., Lori, N.F., Cull, T.S., Akbudak, E., Snyder, A.Z., Shimony, J.S., McKinstry, R.C., Burton, H., and Raichle, M.E. (1999). Tracking neuronal fiber pathways in the living human brain. *Proc. Natl. Acad. Sci. USA* 96, 10422–10427.

Cowey, A. (1964). Projection of the retina on to striate and prestriate cortex in the squirrel monkey, *Saimiri sciureus*. *J. Neurophysiol.* 27, 366–393.

d'Avossa, G., Tosetti, M., Crespi, S., Biagi, L., Burr, D.C., and Morrone, M.C. (2007). Spatiotopic selectivity of BOLD responses to visual motion in human area MT. *Nat. Neurosci.* 10, 249–255.

Daniel, P.M., and Whitteridge, D. (1961). The representation of the visual field on the cerebral cortex in monkeys. *J. Physiol.* 159, 203–221.

DeSouza, J.F., Dukelow, S.P., and Vilis, T. (2002). Eye position signals modulate early dorsal and ventral visual areas. *Cereb. Cortex* 12, 991–997.

DeYoe, E.A., Carman, G.J., Bandettini, P., Glickman, S., Wieser, J., Cox, R., Miller, D., and Neitz, J. (1996). Mapping striate and extrastriate

visual areas in human cerebral cortex. *Proc. Natl. Acad. Sci. USA* 93, 2382–2386.

Di Russo, F., Martinez, A., Sereno, M.I., Pitzalis, S., and Hillyard, S.A. (2002). Cortical sources of the early components of the visual evoked potential. *Hum. Brain Mapp.* 15, 95–111.

Dougherty, R.F., Ben-Shachar, M., Bammer, R., Brewer, A.A., and Wandell, B.A. (2005). Functional organization of human occipital-callosal fiber tracts. *Proc. Natl. Acad. Sci. USA* 102, 7350–7355.

Dougherty, R.F., Koch, V.M., Brewer, A.A., Fischer, B., Modersitzki, J., and Wandell, B.A. (2003). Visual field representations and locations of visual areas V1/2/3 in human visual cortex. *J. Vis.* 3, 586–598.

Dukelow, S.P., DeSouza, J.F., Culham, J.C., van den Berg, A.V., Menon, R.S., and Vilis, T. (2001). Distinguishing subregions of the human MT+ complex using visual fields and pursuit eye movements. *J. Neurophysiol.* 86, 1991–2000.

Dumoulin, S.O., Bittar, R.G., Kabani, N.J., Baker, C.L., Jr., Le Goualher, G., Bruce Pike, G., and Evans, A.C. (2000). A new anatomical landmark for reliable identification of human area V5/MT: A quantitative analysis of sulcal patterning. *Cereb. Cortex* 10, 454–463.

Dumoulin, S.O., Hoge, R.D., Baker, C.L., Jr., Hess, R.F., Achtman, R.L., and Evans, A.C. (2003). Automatic volumetric segmentation of human visual retinotopic cortex. *Neuroimage* 18, 576–587.

Dumoulin, S.O., and Wandell, B.A. (2007). Population receptive field estimates in human visual cortex. *Neuroimage*, in press. Published online September 29, 2007. 10.1016/j.neuroimage.2007.09.034.

Eickhoff, S., Walters, N.B., Schleicher, A., Kril, J., Egan, G.F., Zilles, K., Watson, J.D., and Amunts, K. (2005). High-resolution MRI reflects myeloarchitecture and cytoarchitecture of human cerebral cortex. *Hum. Brain Mapp.* 24, 206–215.

Ejima, Y., Takahashi, S., Yamamoto, H., Fukunaga, M., Tanaka, C., Ebisu, T., and Umeda, M. (2003). Interindividual and interspecies variations of the extrastriate visual cortex. *Neuroreport* 14, 1579–1583.

Engel, S.A., Glover, G.H., and Wandell, B.A. (1997). Retinotopic organization in human visual cortex and the spatial precision of functional MRI. *Cereb. Cortex* 7, 181–192.

Engel, S.A., Rumelhart, D.E., Wandell, B.A., Lee, A.T., Glover, G.H., Chichilnisky, E.J., and Shadlen, M.N. (1994). fMRI of human visual cortex. *Nature* 369, 525.

Felleman, D.J., and Van Essen, D.C. (1991). Distributed hierarchical processing in the primate cerebral cortex. *Cereb. Cortex* 1, 1–47.

Fischl, B., and Dale, A.M. (2000). Measuring the thickness of the human cerebral cortex from magnetic resonance images. *Proc. Natl. Acad. Sci. USA* 97, 11050–11055.

Fishman, R.S. (1997). Gordon Holmes, the cortical retina, and the wounds of war. The seventh Charles B. Snyder Lecture. *Doc. Ophthalmol.* 93, 9–28.

Fize, D., Vanduffel, W., Nelissen, K., Denys, K., Chef d'Hotel, C., Faurgas, O., and Orban, G.A. (2003). The retinotopic organization of primate dorsal V4 and surrounding areas: A functional magnetic resonance imaging study in awake monkeys. *J. Neurosci.* 23, 7395–7406.

Fox, P.T., Miezin, F.M., Allman, J.M., Van Essen, D.C., and Raichle, M.E. (1987). Retinotopic organization of human visual cortex mapped with positron-emission tomography. *J. Neurosci.* 7, 913–922.

Friston, K.J., Rotshtein, P., Geng, J.J., Sterzer, P., and Henson, R.N. (2006). A critique of functional localisers. *Neuroimage* 30, 1077–1087.

Galletti, C., Fattori, P., Battaglini, P.P., Shipp, S., and Zeki, S. (1996). Functional demarcation of a border between areas V6 and V6A in the superior parietal gyrus of the macaque monkey. *Eur. J. Neurosci.* 8, 30–52.

Galletti, C., Fattori, P., Gamberini, M., and Kutz, D.F. (1999). The cortical visual area V6: Brain location and visual topography. *Eur. J. Neurosci.* 11, 3922–3936.

Gardner, J.L., Sun, P., Waggoner, R.A., Ueno, K., Tanaka, K., and Cheng, K. (2005). Contrast adaptation and representation in human early visual cortex. *Neuron* 47, 607–620.

Gattass, R., Nascimento-Silva, S., Soares, J.G.M., Lima, B., Jansen, A.K., Diogo, A.C.M., Farias, M.F., Marcondes, M., Botelho, E.P., Mariani, O.S., et al. (2005). Cortical visual areas in monkeys: Location, topography, connections, columns, plasticity and cortical dynamics. *Phil. Trans. R Soc. Lond. B Biol. Sci.* 1629, 709–731.

Gattass, R., Sousa, A.P., and Gross, C.G. (1988). Visuotopic organization and extent of V3 and V4 of the macaque. *J. Neurosci.* 8, 1831–1845.

Goodale, M.A., and Milner, A.D. (1992). Separate visual pathways for perception and action. *Trends Neurosci.* 15, 20–25.

Goossens, J., Dukelow, S.P., Menon, R.S., Vilis, T., and van den Berg, A.V. (2006). Representation of head-centric flow in the human motion complex. *J. Neurosci.* 26, 5616–5627.

Grill-Spector, K., Kushnir, T., Edelman, S., Avidan, G., Itzhak, Y., and Malach, R. (1999). Differential processing of objects under various viewing conditions in the human lateral occipital complex. *Neuron* 24, 187–203.

Grill-Spector, K., Kushnir, T., Hendler, T., Edelman, S., Itzhak, Y., and Malach, R. (1998). A sequence of object-processing stages revealed by fMRI in the human occipital lobe. *Hum. Brain Mapp.* 6, 316–328.

Grill-Spector, K., and Malach, R. (2004). The human visual cortex. *Annu. Rev. Neurosci.* 27, 649–677.

Grinvald, A. (1985). Real-time optical mapping of neuronal activity: From single growth cones to the intact mammalian brain. *Annu. Rev. Neurosci.* 8, 263–305.

Hadjikhani, N., Liu, A.K., Dale, A.M., Cavanagh, P., and Tootell, R.B.H. (1998). Retinotopy and color sensitivity in human visual cortical area V8. *Nat. Neurosci.* 1, 235–241.

Hagler, D.J., Jr., Riecke, L., and Sereno, M.I. (2007). Parietal and superior frontal visuospatial maps activated by pointing and saccades. *Neuroimage* 35, 1562–1577.

Hagler, D.J., Jr., and Sereno, M.I. (2006). Spatial maps in frontal and prefrontal cortex. *Neuroimage* 29, 567–577.

Halgren, E., Dale, A.M., Sereno, M.I., Tootell, R.B., Marinkovic, K., and Rosen, B.R. (1999). Location of human face-selective cortex with respect to retinotopic areas. *Hum. Brain Mapp.* 7, 29–37.

Hansen, K.A., David, S.V., and Gallant, J.L. (2004). Parametric reverse correlation reveals spatial linearity of retinotopic human V1 BOLD response. *Neuroimage* 23, 233–241.

Hansen, K.A., Kay, K.N., and Gallant, J.L. (2007). Topographic organization in and near human visual area V4. *J. Neurosci.*, in press.

Hasson, U., Harel, M., Levy, I., and Malach, R. (2003). Large-scale mirror-symmetry organization of human occipito-temporal object areas. *Neuron* 37, 1027–1041.

Hasson, U., Levy, I., Behrmann, M., Hendler, T., and Malach, R. (2002). Eccentricity bias as an organizing principle for human high-order object areas. *Neuron* 34, 479–490.

Helmholtz, H. (1896). *Physiological Optics* (New York: Dover Publications).

Henschen, S.E. (1893). On the visual path and centre. *Brain* 16, 170–180.

Holmes, G. (1918). Disturbances of vision by cerebral lesions. *Br. J. Ophthalmol.* 2, 353–384.

Horton, J.C., and Hoyt, W.F. (1991). The representation of the visual field in human striate cortex. *Arch. Ophthalmol.* 109, 816–824.

Hubel, D.H., and Wiesel, T.N. (1965). Receptive Fields and Functional Architecture in Two Nonstriate Visual Areas (18 and 19) of the Cat. *J. Neurophysiol.* 28, 229–289.

- Huk, A.C., Dougherty, R.F., and Heeger, D.J. (2002). Retinotopy and functional subdivision of human areas MT and MST. *J. Neurosci.* 22, 7195–7205.
- Iaria, G., and Petrides, M. (2007). Occipital sulci of the human brain: Variability and probability maps. *J. Comp. Neurol.* 507, 243–259.
- Inouye, T. (1909). *Die Sehstrungen bei Schussverletzungen der kortikalen Sehosphäre* (Leipzig, W.: Engelmann).
- Kanwisher, N., McDermott, J., and Chun, M.M. (1997). The fusiform face area: A module in human extrastriate cortex specialized for face perception. *J. Neurosci.* 17, 4302–4311.
- Kastner, S., De Weerd, P., Pinsk, M.A., Elizondo, M.I., Desimone, R., and Ungerleider, L.G. (2001). Modulation of sensory suppression: Implications for receptive field sizes in the human visual cortex. *J. Neurophysiol.* 86, 1398–1411.
- Kastner, S., DeSimone, K., Konen, C.S., Szczepanski, S.M., Weiner, K.S., and Schneider, K.A. (2007). Topographic maps in human frontal cortex revealed in memory-guided saccade and spatial working-memory tasks. *J. Neurophysiol.* 97, 3494–3507.
- Larsson, J., and Heeger, D.J. (2006). Two retinotopic visual areas in human lateral occipital cortex. *J. Neurosci.* 26, 13128–13142.
- Larsson, J., Landy, M.S., and Heeger, D.J. (2006). Orientation-selective adaptation to first- and second-order patterns in human visual cortex. *J. Neurophysiol.* 95, 862–881.
- Levy, I., Hasson, U., Avidan, G., Hendler, T., and Malach, R. (2001). Center-periphery organization of human object areas. *Nat. Neurosci.* 4, 533–539.
- Li, X., Dumoulin, S.O., Mansouri, B., and Hess, R.F. (2007). The fidelity of the cortical retinotopic map in human amblyopia. *Eur. J. Neurosci.* 25, 1265–1277.
- Liu, J., and Wandell, B.A. (2005). Specializations for chromatic and temporal signals in human visual cortex. *J. Neurosci.* 25, 3459–3468.
- Lyon, D.C., and Kaas, J.H. (2002). Evidence for a modified V3 with dorsal and ventral halves in macaque monkeys. *Neuron* 33, 453–461.
- Malach, R., Levy, I., and Hasson, U. (2002). The topography of high-order human object areas. *Trends Cogn. Sci.* 6, 176–184.
- Malach, R., Reppas, J.B., Benson, R.R., Kwong, K.K., Jiang, H., Kennedy, W.A., Ledden, P.J., Brady, T.J., Rosen, B.R., and Tootell, R.B. (1995). Object-related activity revealed by functional magnetic resonance imaging in human occipital cortex. *Proc. Natl. Acad. Sci. USA* 92, 8135–8139.
- McKeefry, D.J., and Zeki, S. (1997). The position and topography of the human colour centre as revealed by functional magnetic resonance imaging. *Brain* 120, 2229–2242.
- McKyton, A., and Zohary, E. (2007). Beyond retinotopic mapping: The spatial representation of objects in the human lateral occipital complex. *Cereb. Cortex* 17, 1164–1172.
- Merabet, L.B., Swisher, J.D., McMains, S.A., Halko, M.A., Amedi, A., Pascual-Leone, A., and Somers, D.C. (2007). Combined activation and deactivation of visual cortex during tactile sensory processing. *J. Neurophysiol.* 97, 1633–1641.
- Milner, A.D., and Goodale, M.A. (2006). *The Visual Brain in Action*, Second Edition (New York: Oxford University Press).
- Montaser-Kouhsari, L., Landy, M.S., Heeger, D.J., and Larsson, J. (2007). Orientation-selective adaptation to illusory contours in human visual cortex. *J. Neurosci.* 27, 2186–2195.
- Morland, A.B., Baseler, H.A., Hoffmann, M.B., Sharpe, L.T., and Wandell, B.A. (2001). Abnormal retinotopic representations in human visual cortex revealed by fMRI. *Acta Psychol. (Amst.)* 107, 229–247.
- Munk, H. (1881). On the functions of the cortex. In *The Cerebral Cortex*, G. Von Bonin, eds. (Springfield, Illinois: Charles C. Thomas), pp. 97–117.
- Newton, I. (1704). *Opticks: A Treatise of the Reflections Refractions, Inflections and Colours of Light*, 4th Edition (London: Printed for William Innys at the West End of St. Paul's).
- Ogawa, S., and Lee, T.M. (1990). Magnetic resonance imaging of blood vessels at high fields: In vivo and in vitro measurements and image simulation. *Magn. Reson. Med.* 16, 9–18.
- Ogawa, S., Lee, T.M., Nayak, A.S., and Glynn, P. (1990). Oxygenation-sensitive contrast in magnetic resonance image of rodent brain at high magnetic fields. *Magn. Reson. Med.* 14, 68–78.
- Ogawa, S., Tank, D., Menon, R., Ellermann, J., Kim, S., Merkle, H., and Ugurbil, K. (1992). Intrinsic signal changes accompanying sensory stimulation: Functional brain mapping with magnetic resonance imaging. *Proc. Natl. Acad. Sci. USA* 89, 5951–5955.
- Orban, G.A., Dupont, P., De Bruyn, B., Vogels, R., Vandenberghe, R., and Mortelmans, L. (1995). A motion area in human visual cortex. *Proc. Natl. Acad. Sci. USA* 92, 993–997.
- Pakkenberg, B., and Gundersen, H.J. (1997). Neocortical neuron number in humans: Effect of sex and age. *J. Comp. Neurol.* 384, 312–320.
- Pandya, D.N., Seltzer, B., and Barbas, H. (1988). Input-Output organization of the primate cerebral cortex. In *Comparative Primate Biology*, H.D. Staklis and J. Erwin, eds. (New York: Alan R. Liss), pp. 39–80.
- Phillips, C.G., Zeki, S., and Barlow, H.B. (1984). Localization of function in the cerebral cortex. Past, present and future. *Brain* 107, 327–361.
- Pitzalis, S., Galletti, C., Huang, R.S., Patria, F., Committeri, G., Galati, G., Fattori, P., and Sereno, M.I. (2006). Wide-field retinotopy defines human cortical visual area v6. *J. Neurosci.* 26, 7962–7973.
- Press, W.A., Brewer, A.A., Dougherty, R.F., Wade, A.R., and Wandell, B.A. (2001). Visual areas and spatial summation in human visual cortex. *Vision Res.* 41, 1321–1332.
- Qiu, A., Rosenau, B.J., Greenberg, A.S., Hurdal, M.K., Barta, P., Yantis, S., and Miller, M.I. (2006). Estimating linear cortical magnification in human primary visual cortex via dynamic programming. *Neuroimage* 31, 125–138.
- Rademacher, J., Caviness, V.S., Jr., Steinmetz, H., and Galaburda, A.M. (1993). Topographical variation of the human primary cortices: Implications for neuroimaging, brain mapping, and neurobiology. *Cereb. Cortex* 3, 313–329.
- Rosa, M.G., and Tweedale, R. (2005). Brain maps, great and small: Lessons from comparative studies of primate visual cortical organization. *Philos. Trans. R. Soc. Lond. B Biol. Sci.* 360, 665–691.
- Rottschy, C., Eickhoff, S.B., Schleicher, A., Mohlberg, H., Kujovic, M., Zilles, K., and Amunts, K. (2007). Ventral visual cortex in humans: Cytoarchitectonic mapping of two extrastriate areas. *Hum. Brain Mapp.* 28, 1045–1059.
- Russell, G. (2001). Hermann Munk. *Encyclopedia of Life Sciences* (Hoboken, NJ: John Wiley & Sons, Ltd.), p. 1.
- Salzman, C.D., Britten, K.H., and Newsome, W.T. (1990). Cortical microstimulation influences perceptual judgements of motion direction. *Nature* 346, 174–177.
- Salzman, C.D., Murasugi, C.M., Britten, K.H., and Newsome, W.T. (1992). Microstimulation in visual area MT: Effects on direction discrimination performance. *J. Neurosci.* 12, 2331–2355.
- Saxe, R., Brett, M., and Kanwisher, N. (2006). Divide and conquer: A defense of functional localizers. *Neuroimage* 30, 1088–1096.
- Schira, M.M., Wade, A.R., and Tyler, C.W. (2007). Two-dimensional mapping of the central and parafoveal visual field to human visual cortex. *J. Neurophysiol.* 97, 4284–4295.
- Schluppeck, D., Glimcher, P., and Heeger, D.J. (2005). Topographic organization for delayed saccades in human posterior parietal cortex. *J. Neurophysiol.* 94, 1372–1384.
- Schneider, G.E. (1969). Two visual systems. *Science* 163, 895–902.

- Schneider, W., Noll, D.C., and Cohen, J.D. (1993). Functional topographic mapping of the cortical ribbon in human vision with conventional MRI scanners. *Nature* 365, 150–153.
- Schwartz, E.L. (1977). Spatial mapping in the primate sensory projection: Analytic structure and relevance to perception. *Biol. Cybern.* 25, 181–194.
- Sereno, M.I., Dale, A.M., Reppas, J.B., Kwong, K.K., Belliveau, J.W., Brady, T.J., Rosen, B.R., and Tootell, R.B. (1995). Borders of multiple human visual areas in humans revealed by functional MRI. *Science* 268, 889–893.
- Sereno, M.I., Pitzalis, S., and Martinez, A. (2001). Mapping of contralateral space in retinotopic coordinates by a parietal cortical area in humans. *Science* 294, 1350–1354.
- Shepard, R.N. (1981). Psychophysical complementarity. In *Perceptual Organization*, M. Kubovy and J. Pomerantz, eds. (NJ: Lawrence Erlbaum Associates), pp. 279–341.
- Shepard, R.N. (2001). Perceptual-cognitive universals as reflections of the world. *Behav. Brain Sci.* 24, 581–601.
- Sherman, S.M., and Guillery, R.W. (2001). *Exploring the Thalamus* (San Diego: Academic Press).
- Shipp, S., Watson, J.D., Frackowiak, R.S., and Zeki, S. (1995). Retinotopic maps in human prestriate visual cortex: The demarcation of areas V2 and V3. *Neuroimage* 2, 125–132.
- Silver, M.A., Ress, D., and Heeger, D.J. (2005). Topographic maps of visual spatial attention in human parietal cortex. *J. Neurophysiol.* 94, 1358–1371.
- Sincich, L.C., Park, K.F., Wohlgenuth, M.J., and Horton, J.C. (2004). Bypassing V1: A direct geniculate input to area MT. *Nat. Neurosci.* 7, 1123–1128.
- Smith, A.T., Greenlee, M.W., Singh, K.D., Kraemer, F.M., and Hennig, J. (1998). The processing of first- and second-order motion in human visual cortex assessed by functional magnetic resonance imaging (fMRI). *J. Neurosci.* 18, 3816–3830.
- Smith, A.T., Singh, K.D., Williams, A.L., and Greenlee, M.W. (2001). Estimating receptive field size from fMRI data in human striate and extrastriate visual cortex. *Cereb. Cortex* 11, 1182–1190.
- Smith, A.T., Wall, M.B., Williams, A.L., and Singh, K.D. (2006). Sensitivity to optic flow in human cortical areas MT and MST. *Eur. J. Neurosci.* 23, 561–569.
- Stenbacka, L., and Vanni, S. (2007). fMRI of peripheral visual field representation. *Clin. Neurophysiol.* 118, 1303–1314.
- Stensaas, S.S., Eddington, D.K., and Dobbelle, W.H. (1974). The topography and variability of the primary visual cortex in man. *J. Neurosurg.* 40, 747–755.
- Sunness, J.S., Liu, T., and Yantis, S. (2004). Retinotopic mapping of the visual cortex using functional magnetic resonance imaging in a patient with central scotomas from atrophic macular degeneration. *Ophthalmology* 111, 1595–1598.
- Sutter, E.E., and Tran, D. (1992). The field topography of ERG components in man-I. The photopic luminance response. *Vision Res.* 32, 433–446.
- Swisher, J.D., Halko, M.A., Merabet, L.B., McMains, S.A., and Somers, D.C. (2007). Visual topography of human intraparietal sulcus. *J. Neurosci.* 27, 5326–5337.
- Talairach, J., and Tournoux, P. (1988). *Co-Planar Stereotaxic Atlas of the Human Brain* (New York: Thieme Medical Publishers).
- Talbot, S., and Marshall, W. (1941). Physiological studies on neural mechanisms of visual localization and discrimination. *Am. J. Ophthalmol.* 24, 1255–1263.
- Talbot, S.A. (1940). Arrangement of visual field on cat's cortex. *Am. J. Physiol.* 129, 477–478.
- Talbot, S.A. (1942). A lateral localization in the cat's visual cortex. *Fed. Proc.* 1, 84.
- Teuber, H.L., Battersby, W.S., and Bender, M.B. (1960). *Visual Field Defects After Penetrating Missile Wounds of the Brain* (Cambridge, MA: Harvard University Press).
- Thirion, B., Duchesnay, E., Hubbard, E., Dubois, J., Poline, J.B., LeBihan, D., and Dehaene, S. (2006). Inverse retinotopy: Inferring the visual content of images from brain activation patterns. *Neuroimage* 33, 1104–1116.
- Thompson, J.M., Woolsey, C.N., and Talbot, S.A. (1950). Visual areas I and II of cerebral cortex of rabbit. *J. Neurophysiol.* 12, 277–288.
- Thompson, P.M., Schwartz, C., Lin, R.T., Khan, A.A., and Toga, A.W. (1996). Three-dimensional statistical analysis of sulcal variability in the human brain. *J. Neurosci.* 16, 4261–4274.
- Tootell, R.B., and Hadjikhani, N. (2001). Where is 'dorsal V4' in human visual cortex? Retinotopic, topographic and functional evidence. *Cereb. Cortex* 11, 298–311.
- Tootell, R.B., Hadjikhani, N., Hall, E.K., Marrett, S., Vanduffel, W., Vaughan, J.T., and Dale, A.M. (1998). The retinotopy of visual spatial attention. *Neuron* 21, 1409–1422.
- Tootell, R.B., Mendola, J.D., Hadjikhani, N.K., Ledden, P.J., Liu, A.K., Reppas, J.B., Sereno, M.I., and Dale, A.M. (1997). Functional analysis of V3A and related areas in human visual cortex. *J. Neurosci.* 17, 7060–7078.
- Tootell, R.B., Reppas, J.B., Kwong, K.K., Malach, R., Born, R.T., Brady, T.J., Rosen, B.R., and Belliveau, J.W. (1995). Functional analysis of human MT and related visual cortical areas using magnetic resonance imaging. *J. Neurosci.* 15, 3215–3230.
- Tootell, R.B., and Taylor, J.B. (1995). Anatomical evidence for MT and additional cortical visual areas in humans. *Cereb. Cortex* 5, 39–55.
- Trevarthen, C.B. (1968). Two mechanisms of vision in primates. *Psychol. Forsch.* 37, 299–348.
- Tusa, R.J., Palmer, L.A., and Rosenquist, A.C. (1978). The retinotopic organization of area 17 (striate cortex) in the cat. *J. Comp. Neurol.* 177, 213–235.
- Tyler, C.W., Likova, L.T., Chen, C.-C., Kontsevich, L.L., Schira, M.M., and Wade, A.R. (2005). Extended Concepts of Occipital Retinotopy. *Current Medical Imaging Reviews* 1, 319–329.
- Ungerleider, L.G., and Mishkin, M. (1982). Two Cortical Visual Systems. In *The Analysis of Visual Behavior*, D.J. Ingle, M.A. Goodale, and R.J.W. Mansfield, eds. (Cambridge: MIT Press), pp. 549–586.
- Van Essen, D.C. (2002). Surface-based atlases of cerebellar cortex in the human, macaque, and mouse. *Ann. N Y Acad. Sci.* 978, 468–479.
- Van Essen, D.C. (2003). Organization of Visual Areas in Macaque and Human Cerebral Cortex. In *The Visual Neurosciences*, L.M. Chalupa and J.S. Werner, eds. (Boston: Bradford Books), pp. 507–521.
- Van Essen, D.C. (2005). A Population-Average, Landmark- and Surface-based (PALS) atlas of human cerebral cortex. *Neuroimage* 28, 635–662.
- Van Essen, D.C. (2007). *Evolution of Nervous Systems*. *Neuroimage*, in press.
- Van Essen, D.C., and Maunsell, J.H. (1983). Hierarchical organization and functional streams in the visual cortex. *Trends Neurosci.* 6, 370–375.
- Vanduffel, W., Fize, D., Mandeville, J.B., Nelissen, K., Van Hecke, P., Rosen, B.R., Tootell, R.B., and Orban, G.A. (2001). Visual motion processing investigated using contrast agent-enhanced fMRI in awake behaving monkeys. *Neuron* 32, 565–577.
- Vanni, S., Henriksson, L., and James, A.C. (2005). Multifocal fMRI mapping of visual cortical areas. *Neuroimage* 27, 95–105.

- Victor, J.D., Apkarian, P., Hirsch, J., Conte, M.M., Packard, M., Relkin, N.R., Kim, K.H., and Shapley, R.M. (2000). Visual function and brain organization in non-decussating retinal-fugal fibre syndrome. *Cereb. Cortex* 10, 2–22.
- Wade, A.R., Brewer, A.A., Rieger, J.W., and Wandell, B.A. (2002). Functional measurements of human ventral occipital cortex: Retinotopy and colour. *Philos. Trans. R. Soc. Lond. B Biol. Sci.* 357, 963–973.
- Wakana, S., Jiang, H., Nagae-Poetscher, L.M., van Zijl, P.C., and Mori, S. (2004). Fiber tract-based atlas of human white matter anatomy. *Radiology* 230, 77–87.
- Wandell, B.A. (1995). *Foundations of Vision* (Sunderland, MA: Sinauer Press).
- Wandell, B.A., Brewer, A.A., and Dougherty, R.F. (2005). Visual field map clusters in human cortex. *Philos. Trans. R. Soc. Lond. B Biol. Sci.* 360, 693–707.
- Wandell, B.A., Dumoulin, S.O., and Brewer, A.A. (2006). Computational neuroimaging: Color signals in the visual pathways. *Neuro-ophthalmol. Jpn.* 23, 324–343.
- Wandell, B.A., Dumoulin, S.O., and Brewer, A.A. (2007). Visual cortex in humans. In *The New Encyclopedia of Neuroscience*, L. Squire, et al., eds. (Oxford, England: Elsevier), In press.
- Warnking, J., Dojat, M., Guerin-Dugue, A., Delon-Martin, C., Olympieff, S., Richard, N., Chehikian, A., and Segebarth, C. (2002). fMRI retinotopic mapping—step by step. *Neuroimage* 17, 1665–1683.
- Watson, J.D., Myers, R., Frackowiak, R.S., Hajnal, J.V., Woods, R.P., Mazziotta, J.C., Shipp, S., and Zeki, S. (1993). Area V5 of the human brain: Evidence from a combined study using positron emission tomography and magnetic resonance imaging. *Cereb. Cortex* 3, 79–94.
- Wilms, M., Eickhoff, S.B., Specht, K., Amunts, K., Shah, N.J., Malikovic, A., and Fink, G.R. (2005). Human V5/MT+: Comparison of functional and cytoarchitectonic data. *Anat. Embryol. (Berl.)* 210, 485–495.
- Wohlschlagel, A.M., Specht, K., Lie, C., Mohlberg, H., Wohlschlagel, A., Bente, K., Pietrzyk, U., Stocker, T., Zilles, K., Amunts, K., and Fink, G.R. (2005). Linking retinotopic fMRI mapping and anatomical probability maps of human occipital areas V1 and V2. *Neuroimage* 26, 73–82.
- Yoshor, D., Bosking, W.H., Ghose, G.M., and Maunsell, J.H. (2007). Receptive fields in human visual cortex mapped with surface electrodes. *Cereb. Cortex* 17, 2293–2302.
- Young, M.P. (1992). Objective analysis of the topological organization of the primate cortical visual system. *Nature* 358, 152–155.
- Zeki, S. (1990). Parallelism and Functional Specialization in Human Visual Cortex. *Cold Spring Harb. Symp. Quant. Biol.* 55, 651–661.
- Zeki, S. (1993). *A Vision of the Brain* (London: Blackwell Scientific Publications).
- Zeki, S. (2003). Improbable areas in the visual brain. *Trends Neurosci.* 26, 23–26.
- Zeki, S., Watson, J.D., Lueck, C.J., Friston, K.J., Kennard, C., and Frackowiak, R.S. (1991). A direct demonstration of functional specialization in human visual cortex. *J. Neurosci.* 11, 641–649.
- Zeki, S.M. (1969). Representation of central visual fields in prestriate cortex of monkey. *Brain Res.* 14, 271–291.
- Zeki, S.M. (1971). Convergent input from the striate cortex (area 17) to the cortex of the superior temporal sulcus in the rhesus monkey. *Brain Res.* 28, 338–340.
- Zeki, S.M. (1976). The projections to the superior temporal sulcus from areas 17 and 18 in rhesus monkey. *Proc. R. Soc. Lond. B. Biol. Sci.* 193, 119–207.